

# About the return period of a catastrophe

Mathias Raschke<sup>1</sup>

<sup>1</sup>Freelancer/independent researcher, Stolze-Schrey-Str.1, 65195 Wiesbaden, Germany

Correspondence to: Mathias Raschke (mathiasraschke@t-online.de.com)

5 **Abstract.** ~~To understand catastrophes like earthquakes stochastically, When a natural hazard event like an earthquake affects a region and generates a natural catastrophe (NatCat), the following questions arise: How often does such an event occurs? What is their return period (RP) should be quantified for the concerned region. Measures such as event magnitudes or indexes are less helpful for this purpose.?)~~ We derive the combined return period (CRP) from a concept of extreme value statistics and theory - the pseudo-polar coordinates of extreme value theory. The A CRP is the (weighted) meanaverage of the local RPs  
10 and is again an RP; other metrics do not provide such testable reproducibility. We demonstrate CRP's opportunities on extratropical cyclones (winter storms) over Germany, including validation and bias correction of local RP estimates. Furthermore, we introduce new estimation methods for the RP of an event loss (risk curve) via CRP scaling of historical storm fields. For high RP, the resulting event losses of the German insurance market are higher in the case of max-stable dependence. The latter means the same dependence level between local maxima of a year as of a decade. However, intensities. Since CRP's  
15 reciprocal is its expected exceedance frequency, which applies to any RP per stochastic definition, the concept is testable. As we show, the CRP is related to the spatial dependence is not stable but decreases by increasing period. Such control of characteristic of the NatCat generating hazard event and their spatial dependence is not realized by of corresponding local block maxima (e.g., annual wind speed maximum). For this purpose, we extend previous risk models construction for max-stable random fields from science and industry. Our loss estimates for RP of 200 years are extreme value theory and consider  
20 a recent concept from NatCat research. Based on the CRP, we also significantly smaller than those of European regulation's standard model develop a new method to estimate the NatCat risk of a region via stochastic scaling of historical fields of local event intensities (represented by records of measuring stations) and averaging corresponding risk parameters such as the event loss with a defined RP.

Our application example is winter storm (extratropical cyclones) over Germany. We analyze wind station data and estimate  
25 local hazard, CRP of historical events and the risk curve of insured event losses. The most destructive storm of our observation period of 20 years is Kyrill 2002 with weighted CRP  $16.97 \pm 1.75$ . The CRPs could be successfully tested statistically. We also state that our risk estimate is higher for the max-stable case than for the non-max-stable. Max-stable means that the dependence measure (e.g., Kendall's  $\tau$ ) for annual wind speed maxima of two wind stations has the same value as for maxima of higher block size such 10 or 100 years since the copula (the dependence structure) remains the same. However, the spatial dependence  
30 decreases with increasing block size; a new statistical indicator confirms this. Such control of spatial characteristic and dependence is not realized by the previous risk models in science and industry. We compare our risk estimates to these.

# 1 Introduction

35 ~~When~~After a natural ~~catastrophe (NatCat)~~hazard event such as a large windstorm or an earthquake has occurred, in a defined region (e.g., in a country) and results in a natural catastrophe (NatCat), the question arises, how ~~often~~does such random ~~event~~event appear, i.e.,? What is the corresponding return period (RP, also called recurrence interval)? Before discussing this issue, we underline that the extension of river ~~floods~~flood events or windstorms in time and space depend on the scientific and socio-economic event definition. ~~These are~~The definitions may vary by peril and is not our topic even though they influence our research object – the RP of a hazard and NatCat event.

40 The RP of an event magnitude or index is so far frequently used as a stochastic measure of a catastrophe. For example, there are different magnitudes scales for earthquakes (Bormann and Saul, 2009). ~~Unfortunately, corresponding RPs for the source region~~But their RP may not correspond well with the ~~catastrophe~~local consequences since the ~~hypo~~centre~~hypo~~center position also determines ~~destructiveness~~local event intensities and effects. For floods, regional or global magnitude scales are not in use (Guse et al., 2020). For hurricanes, the Saffir–Simpson scale (National Hurricane Centre, 2020) is a magnitude measure; but the random storm track also influences the ~~destruction's~~ extent of ~~the~~ destruction. Extratropical cyclones hitting 45 Europe, called winter storms, are measured by a storm severity index (SSI; Roberts et al., 2014) or extreme wind index (EWI; Della-Marta et al., 2009). Their different definitions result in quite different RP for the same events. ~~Also, their statistical models include assumptions and pitfalls.~~In rare scientific publications about risk ~~modeling~~modelling for the insurance industry, such as by ~~Mitchell~~Mitchell-Wallace et al. (2017), better and universal approaches for the RP are not offered. In sum, previous approaches are not very fruitful. ~~Nevertheless, RP is needed to understand and manage NatCat risk by decision-makers in administration, policy, and industry and research the consequences of climate change (Della Marta et al. 2010, Schwierz et al. 2010). In the end, the RP of losses and damage (the risk curve) is needed~~successful regarding the stochastic quantification of a hazard or NatCat event what our motivation is to develop a new approach. We mathematically derive the concept of combined return period (CRP) being the average of RPs of local event intensities from an approach of extreme value theory and statistics. As we will show by a combination of previous and new approaches from stochastic and NatCat research, the concept of CRP is strongly related to the spatial association/dependence between the local event intensities, their RPs, and corresponding block maxima such as annual maxima.

60 This spatial dependence is less or inappropriately considered in previous research about NatCat. The issue is only a marginal topic in the book about NatCat modelling for insurance industry by Mitchell-Wallace et al. (2017, Section 5.4.2.5). Jongman's et al. (2014) model for European flood risk considers such dependence explicitly. However, their assumptions and estimates are not appropriate according to Raschke (2015). In statistical journals, max-stable dependence models have been applied to natural hazards without a systematic test of the stability assumption, such as the snow model by Blanchet and Davison (2011) for Switzerland and the river flood model by Asadi et al. (2015) for the Upper Danube River system. Max-stable dependence means that the copula (the dependence structure of a bi- or multivariate distribution) and corresponding value of dependence measures are the same for annual maxima as for ten-year maxima or these of a century (Dey et al., 2016).

65 Raschke's et al. (2011) winter storm risk model for a power transmission grid in Switzerland also implies this stability assumption without a validation. The sophisticated model for spatial dependence between local river floods by Keef et al. (2009) is very flexible. However, it needs a high number of parameters, and the spatial dependence cannot be simply interpolated as it is possible with covariance and correlation functions (Schabenberger and Gotway, 2005, Section 2.4). Youngman and Stephenson (2016) suggested a statistical modelling and simulation for hazard events. As far as we understand,  
70 they generate wind fields by a Monte Carlo simulation of a complex random field. However, the random occurrence of a hazard event is more like a point event of a Poisson process than the draw/realization of a random variable. An example illustrates the difference: the random variable *local annual loss from catastrophes* is realized every year even though not one catastrophe and loss event need to be occurred. The same concern applies to the idea by Papalexioiu et al. (2021) for storm simulation. In the research of spatial dependence by Bonazzi et al. (2012) and Dawkins and Stephenson (2018), the local  
75 extremes of European winter storms are sampled by a pre-defined list of significant events. For these reasons, at first, we derive from extreme value theory a flexible and reproductive stochastic measure for a NatCat in a defined region—the combined return period (CRP). Then, we explain implications and opportunities in section 2. These are testability, scalability, and a variant of Raschke's (2013) area function. We apply the concepts to extratropical cyclones (winter storms) in Germany, estimate the CRP for historical events of last decades, and test the CRP concept. Since the CRP is spatial related, we also  
80 examine spatial dependence between local hazards. Furthermore, we use the derived scaling opportunity of historical event fields to estimate a risk curve for the aggregate of insured losses per event in Germany in consideration of loss data. In section 3, we explain statistical details of the analysis of German winter storms regarding local hazard, vulnerability, and uncertainties. Subsequently, we present stochastic interpretations and numerical details of the risk estimate. Finally, in section 5, we summarize and discuss our results with a focus on previous analysis of risk and spatial dependence.

## 85 **2 Theory and Application of CRP**

### **2.1 Derivation of CRP**

Stochastic deals with more than only random variables. A Poisson point process or briefly Poisson process (Coles, 2001; Beirlant et al., 2004; Falk et al. 2011) Such sampling is not foreseen in (multivariate) extreme value statistics; block maxima and (declustered) POT are the established sampling methods (Coles, 2010, Section 3.4 and 4.4; Beirlant et al., 2004, Section  
90 9.3, 9.4).

Event wise spatial sampling is also a random element with random point events a critical task; the variable time lag between the occurrences at different measuring station, such as river gauging stations, makes it confusing. The corresponding assignment of Asadi et al. (2015) of one local flood peak to peaks at the line of real numbers. A NatCat event other sites does not convince us completely. The same applies to Jongman et al. (2014; Raschke, 2015b). The sampling of multivariate block  
95 maxima is measured by its simpler. However, the univariate sampling and analysis is also not trivial as interpretations of the

trend in time series of a wind station in Potsdam (Germany) over several decades shows. Wichura (2009) assumes changed local roughness condition over the time as reason, Mudelsee (2020) the climate change.

The research of spatial dependence of natural hazards is not an end in itself, the final goal is an answer to the question about the NatCat risk. What is the RP of events with aggregate damage or losses in a region equal or higher to a defined level? By using CRP, we quantify the risk via stochastic scaling of fields of local intensity (e.g., river discharge or wind gust peak) at a geographical site-intensities of historical events and averaging corresponding risk measures. This local intensity occurs (approximately) as point event of a Poisson process with points  $X$ ; the number of independent new approach significantly extends the methods to calculate a NatCat risk curve. Previous opportunities for a risk estimate are the conventional statistical models that are fitted to observed or re-analyzed aggregated losses (also called as-if losses; ) of historical events as used by Donat et al. (2011) and by Pfeifer (2010) for annual sums. The advantages of such simple models are the controlled stochastic assumptions and the small number of parameters; the disadvantages are high uncertainty for widely extrapolated values and limited opportunities to consider further knowledge. The NatCat models in (re)insurance industry combine different components/sub-models for hazard, exposure (building stock or insured portfolio) and corresponding vulnerability (Mitchell-Wallace et al. 2017, Section 1.8; Raschke, 2018) and offers better opportunities for knowledge transfer such as the differentiated projection of a market model on a single insurer. However, the corresponding standard error of the risk estimates is frequently not quantified (and cannot be quantified). The numerical burden of such complex models is high. Tens of thousands of NatCat events must be simulated (Mitchell-Wallace et al., 2017, Chapter 1). The question arises, what is the stochastic criterion for the simulation of a reasonable event set in NatCat modelling? As far as we know, scientific NatCat models for European winter storms (extratropical cyclones) are based on numerical simulations (Della-Marta et al., 2010; Schwierz et al., 2010; Osinski et al., with  $X \geq x$  during a defined unit period (e.g., a season or a year) is a random integer number  $K$  that follows a Poisson-2016) and are not intensively validated regarding spatial dependence.

To answer our questions, we start with topics of extreme value statistics in the 2<sup>nd</sup> Section and illuminate max-stability in the univariate sense, for the dependence structure (copula) of the bivariate case and max-stable random fields. We also extend Schlather's (2002) 1<sup>st</sup> theorem with focus on spatial dependence. The more recent approaches of hazard event related area functions (Raschke, 2013) and survival functions (Jung and Schindler, 2019) of local event intensities within a region are implemented therein to characterize spatiality. In the 3<sup>rd</sup> Section, we derive the CRP from the concept of pseudo polar coordinates of extreme value statistics and explain its testability and scaling opportunity and corresponding risk estimate. Subsequently, in Section 4, we apply the new approaches to winter storms (extratropical cyclones) over Germany to demonstrate their potentials. This application implies several elements of conventional statistics which are explained in Section 5. Finally, we summarize and discuss our results and give an outlook in Section 6. Some stochastic and statistical details are presented in the Supplementary and Supplementary Data to remain clarity of the main paper and limit its extent. In the entire paper, we must consider several stochastic relations. Therefore, the same mathematical symbol can have different meanings in different subSections. We also expect that the reader is more familiar with statistics and stochastic than only with basics

130 about random variables. Statistical significance, goodness-of-fit tests, random fields, or a Poisson (point) process (Upton and Cook, 2008) should be familiar terms.

## 2 Max-stability in statistics and stochastic

### 2.1 The univariate case

135 Before we formulate the CRP and discuss their opportunities, we must present, discuss, and extend a corresponding topic – max-stability in extreme value statistics especial of random process and fields. Max-stability has its origin in univariate statistics. The cumulative distribution functions (CDF)  $F_n(x)$  of maximum  $X_n = \text{Max}(X_1, \dots, X_n)$  of  $n$  identical and independently distributed (iid) random variables  $X_i$  with CDF  $F(x)$  (for the non-exceedance probability  $\text{Pr}(X \leq x)$ ) is

$$F_n(x) = F(x)^n \quad (1)$$

A CDF  $F(x)$  is max stable if the linear transformed maximum (with parameters  $a_n$  and  $b_n$ ) has the same distribution (Coles, 2001, Def. 3.1)

140  $F_n(a_n x + b_n) = F(a_n x + b_n)^n = F(x) \quad (2)$

The Fréchet distribution (Beirlant et al., 2004; Falk et al., Tab. 2.1) is such a max-stable distribution, also called extreme value distribution, with CDF

$$G(x) = \exp\left(-\frac{1}{x^\alpha}\right), x \geq 0, \alpha > 0 \quad (3)$$

145 For the unit Fréchet distribution is  $\alpha = 1$  and the transformation parameters are  $b_n = 0$  and  $a_n = n$ . The most distribution types are not max-stable, but their distribution of maxima (1) converges to an extreme value distribution by increasing sample size  $n$ , called the block size in this context (Beirlant et al., 2004, Chapter 3). These are well-known facts, and we can only refer to some of a very high number of corresponding publications (e.g., de Haan and Ferrira, 2007; Falk et al. 2011) with an). Coles (2001) gives a good overview for practitioners.

### 2.2 Max-stable copulas

150 It is also well-known that a bivariate CDF  $F(x, y)$  can replace by a copula  $C(u, v)$  and the marginal CDFs  $F_x(x)$  and  $F_y(y)$

$$F(x, y) = C\left(F_x(x), F_y(y)\right) = \text{Pr}(X \leq x, Y \leq y) \quad (4)$$

The copula approach represents a universal distinction between the marginal distributions and the dependence structure and was introduced by Sklar (1959). As there are different univariate distributions (types) there are different copulas (types). Mari and Kotz (2001) presents a good overview about copulas, their construction principals, and different views on dependence. Max-stability is also a property of some copulas, called max-stable copula or extreme copula. A max-stable copula remains the same for pairs of component wise maxima  $(X_n, Y_n)$  as it was already for the underlying pairs  $(X, Y)$ ; the copula parameters including dependence measure such as Kendall's rank correlation are equal. The formal definition is (Dey et al., 2016, (2.3))

$$C_n(u, v) = C(u^{1/n}, v^{1/n})^n \quad (5)$$

160 **2.3 Max-stability of stochastic processes**

The spatial extension of the bivariate situation and corresponding distribution is the random field  $Z(x)$  at points  $x$  in the space  $\mathbb{R}^d$  with  $d$  dimensions (e.g., Schlather, 2001). In our application,  $\mathbb{R}^2$  is the geographical space and  $x$  is the corresponding coordinate vector. At one point/site  $x$  in  $\mathbb{R}^d$ ,  $F_x(z)$  is the marginal distribution of the local random variable  $Z$ . There are various differentiations and variants such as (non)stationarity or (non)homogeneity. A max-stable random field has max-stable marginal distributions and the copulas between to margins are also max-stable. Schlather (2002) has formulated and proofed a construction of a max stable random field (we cite his 1<sup>st</sup> theorem with the same notation)

165 **Theorem 1:** *Let  $Y$  be a measurable random function and  $\mu = \mathbb{E} \int_{\mathbb{R}^d} \max\{0, Y(x)\} dx \in (0, \infty)$ . Let  $\Pi$  be a Poisson process on  $\mathbb{R}^d \times (0, \infty)$  with intensity measure  $d\Lambda(y, s) = \mu^{-1} dy s^{-2} ds$ , and  $Y_{y,s}$  i.i.d. copies of  $Y$ ; then*

$$Z(x) = \sup_{(y,s) \in \Pi} s Y_{y,s}(x - y) = \sup_{(y,s) \in \Pi} s \max\{Y_{y,s}(x - y), 0\}, \quad (6)$$

170 *is a stationary max-stable process with unit Fréchet margins.*

Extreme value statistics is interested in the max-stable dependence structure (copula) between the margins, the unit Fréchet distributed random variables  $Z$  at fixed points  $x$  in space  $\mathbb{R}^d$ . From perspective of NatCat modelling in the geographical space  $\mathbb{R}^2$  and with  $Y(x) \geq 0$ , the entire generating process is interesting. The Poisson (point) process  $\Pi$  represents all hazard events (e.g., storms) of a unit period such as a hazard season or a year and has two parts,  $s$  and  $y$ . The point events  $s$  on  $(0, \infty)$  are a stochastic event magnitude and scale the field of local events intensity  $s_x(x)$ , short called intensity

$$s_x(x) = s Y_{y,s}(x - y) \quad (7)$$

175 which represents all point events  $s_x(x)$  at sites  $x$ . The random coordinate  $y$  is a kind of epicenter in the meaning of NatCat with the (tentiously) highest local event intensity such as maximum wind speed, maximum hail stone diameter, or peaks of earthquake ground accelerations. The copied random function  $Y(x)$  determines the pattern of a single random event in the space  $\mathbb{R}^d$ .  $Y(x)$  or its local expectation (converges to 0 or is 0 if magnitude  $\|x\|$  of coordinate vector converges to infinity due to the measurability condition in Theorem 1. This also applies to NatCat events with limited geographical extend.

185 Schlather (2002) has demonstrated the flexibility of his construction by presenting realizations of maximum fields for different variants of  $Y(x)$ . Its measurability condition is fulfilled by classical probability density functions (PDF, first derivative of the CDF, Coles, 2001, Section 2.2) of random variables. For instance, Smith (1990, an unpublished and frequently cited paper) used the PDF of the normal distribution. We present in the Supplementary, Section 4, some examples of the random function  $Y(x)$  to illustrate the universality of the approach.  $Y(x)$  can also imply random parameters such as verities of standard deviation of applied PDF or is combined with a random field.

Both,  $s$  and  $s_x(x)$  with fixed  $x$ , are point events of Poisson processes with intensity  $s^{-2}ds$ . This is the expected value  $E[\dots]$ —point density and determines the exceedance frequency (EF) function (with  $\Lambda(z)$ ). The latter is the expected number of point events  $s_x(x) > z$  and  $s > z$

$$\Lambda(z) = \int_z^\infty s^{-2} ds = 1/z. \quad (8)$$

The entire construction of Theorem 1 is also a kind of shot noise field according to the definitions of Dombry (2012); and Schlather (2002) has also published a construction of max-stable random field without a random function but with a stationary random field. The logarithmic variant of Theorem 1 (logarithm of (6,7)) also results in a max-stable random field, however, the marginal maxima are unit Gumbel distributed and (8) would be an exponential function. The Brown-Resnick process - well-known in stochastic (e.g., Engelke et al., 2011) - determines a max-stable random field with such unit Gumbel distributions and use a nonstationary random field. It is implicitly a construction according to Theorem 1 since for exponential transformation (inverse of logarithmic transformation) the nonstationary random field is the random function of Theorem 1. The origin of a Brown-Resnick process in  $\mathbb{R}^d$  can be fixed but can also be a random coordinate as  $y$  is in Theorem 1.

The construction of Theorem 1 is already used to model natural hazards in the geographical space. Smith (1990) has applied the bivariate normal distribution as  $Y(x)$  in a rainstorm modelling. The Brown-Resnick Process has been already applied to river flood (Asadi et al., 2015). Blanchet and Davison (2011) have applied a max-stable model for snow and Raschke et al. (2011) for winter storm, both in Switzerland. And there are similarities to conventional hazard models. Punge's et al. (2014) hail simulation includes maximum hail stone diameter that acts like  $\ln(s)$  in (6.7). Raschke (2013) already stated similarity between earthquake ground motion models and Schlather's construction. However, the earthquake magnitude can have a wider influence on the geographical event pattern than a simple scaling. This was one of the motivations to extend and generalize the Schlather's construction (7) with dimension  $d$  of  $\mathbb{R}^d$

$$s_x(x) = s^{1+\beta} Y_{y,s} \left( \left( (1+\beta)s^{-\beta} \right)^{-\frac{1}{d}} (x-y) \right), \beta > -1 \quad (9)$$

And for the corresponding field of maxima (6) we write

$$Z(x) = \sup_{(y,s) \in \Pi} s^{1+\beta} Y_{y,s} \left( \left( (1+\beta)s^{-\beta} \right)^{-\frac{1}{d}} (x-y) \right), \beta > -1 \quad (10)$$

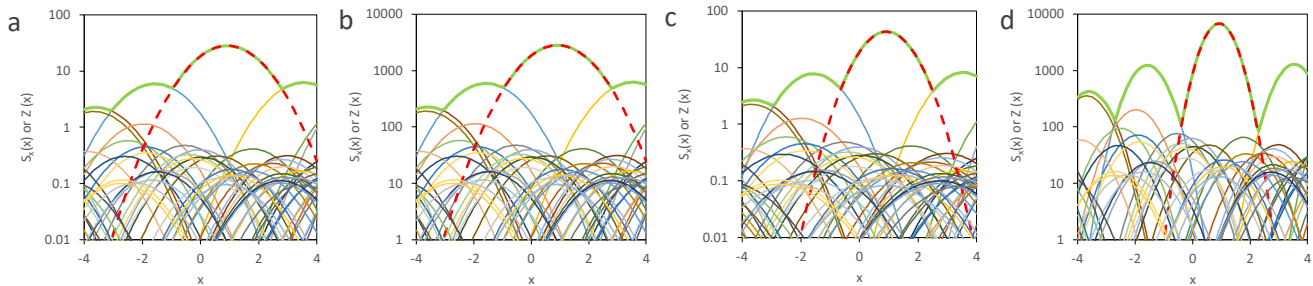
As we show in the Supplementary, Section 2, the marginal Poisson processes  $s_x(x)$  in (9) have the same exceedance frequency (8) as (7). Correspondingly,  $Z(x)$  in (10) is also unit Fréchet distributed as in (6). Schlather's construction is a special case of (9,10) with  $\beta = 0$ ; (9,10) only implies max stability of spatial dependence in this case, what we discuss in the following Section.

#### **2.4 Spatial characteristics and dependence**

We now illustrate spatial max-stability and its absence by examples of (9, 10) with standard normal PDF as random function  $Y(x)$  in a one-dimensional parameter space  $\mathbb{R}^{d=1}$ . For this purpose, we apply the simulation approach of Schlather (2002) and

220 generate random events within a range  $(-10,10)$  for local event intensities within the region/range  $(-4,4)$  in  $\mathbb{R}^1$  by a Monte Carlo simulation. According to Schlather's procedure that processes a series of random numbers from a (pseudo) random generator, only the events for the large  $s$  are simulated which implies incompleteness for smaller events. This does not significantly affect the simulated field  $Z(x)$  of maxima. However, we can only consider this simulation for  $\beta \geq 0$  in (9.10) since the edge effects increase for increasing  $s$  if  $\beta < 0$ . In Figure 1 a, we show fields for one realization  $\Pi$  of Schlather's theorem ( $n = 1$ , equivalent to one year or one season in NatCat modelling) for the max-stable case with  $\beta = 0$  in (9.10). With the same series of random numbers, we generate fields of  $n = 100$  realizations of  $\Pi$  in Figure 1b. It has the same pattern  $n = 1$  and is the same when we linear transform the local intensities  $s_x$  with division by  $n = 100$ . The entire generating processes are max-stable as the resulting marginals and dependence and association/dependence between marginals are. In contrast to this total max-stability, the example with  $\beta = 0.1$  results in different pattern for  $n = 1$  and  $n = 100$  in Figure 1 c and d. The shape of the event fields gets sharper for larger  $s$ , only the marginals are max-stable, not their spatial relations.

230 To illustrates the effect on spatial dependence quantitatively, we have generated local maxima  $Z(x)$  from (10) by Monte Carlo simulation with 100,000 repetitions and computed corresponding dependence measure Kendall's  $\tau$  (Kendall, 1938; Mari and Kotz, 2001, Section 6.2.6). As depicted in Figure 2 a and b, the functions are the same if  $\beta = 0$  and differs if  $\beta = 0.1$ , the dependence is decreasing by increasing  $n$  if  $\beta > 0$ . In Figure 2c, the functions are shown for the limit cases full dependence with the same value of  $s_x(x)$  at each point  $x$  and full independence with  $s_x(x) = 0$  everywhere except one point.



235 **Figure 1: Examples of simulated fields of local event intensities and enveloping field of maxima (bold green line) generated with standard normal PDF as  $Y(x)$  in (6.7,9,10) and the same series of numbers from pseudo-random generator: a) max-stable and  $n=1$ , b) max-stable and  $n=100$ , c) non max-stable and  $n=1$ , d) non max-stable and  $n=100$ . The strongest event has a broken red line.**

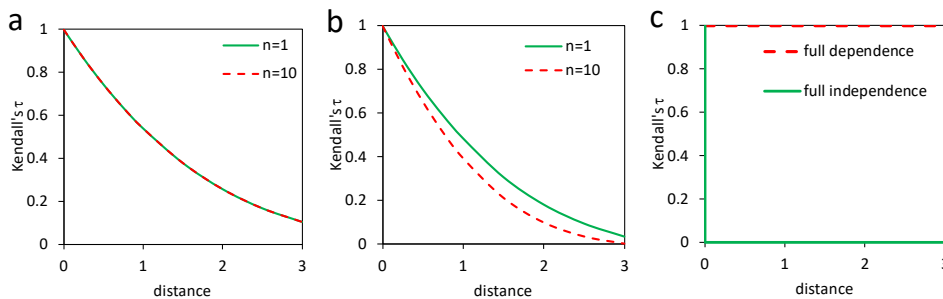




**Figure 2: Spatial dependence in relation to the distance measured by Kendall's  $\tau$ : a) max-stable fields of Figure 1, b) non-max-stable fields of Figure 1, c) limit cases.**

Beside our extension of Schlather's theorem, we also consider a more recent approach from NatCat research to understand the spatial characteristic. Raschke (2013) described an earthquake event by its area function for the peak ground accelerations. This is a cumulative function and measures the set of points in the geographical space (the area) with an event intensity higher than the argument of the function. The area function is limited here to a region and is normalized ( $u$  and  $l$  symbolises the region's bounds, the integral in the denominator is the area of the region in  $\mathbb{R}^2$ ,  $\mathbf{1}$  is an indicator function)

$$A(x) = E[K], K = \sum_{t=1}^{\infty} I(X_t > x).$$

(1)

$$A(z) = \frac{\int_l^u \mathbf{1}(s_x(x) > z) dx}{\int_l^u dx} \quad (11)$$

and is now like a survival function of a random variable (decreasing with value of functions between 0 and 1) which describes the exceedance probability in contrast to a CDF for non-exceedance probability (Upton and Cook, 2008). Jung and Schindler (2019) have already applied such aggregating functions to German winter storm events and call them explicitly survival function. However, not every normalized aggregating decreasing function is based on an actual random variable. And survival functions are not used in statistics to describe regions of random fields or random function as far as we know. Nonetheless, we use the area function (11) to characterize and research the spatiality of the event field  $s_x(x)$  in a defined region. As an example, the area function for the strongest events in Figure 1 is shown in Figure 3 a. The differences between the variants  $n = 1$  versus  $n = 100$  and  $\beta = 0$  versus  $\beta = 0.1$  corresponds with the differences between these events in Figure 1. In Figure 3 b, the limit cases of Figure c are depicted to illustrate the underlying link between area function and spatial dependence.

We also use the parameters of a random variable  $X$  with PDF  $f(x)$  and CDF  $F(x)$  and survival function  $\bar{F}(x) = 1 - F(x)$  to characterize our area function. These parameters are expectation  $E[X]$  (estimated by sample mean/average), variance  $\text{Var}[X]$ , standard deviation  $\text{Sd}[X]$  (the square root of variance), and a coefficient of variation (CV)  $\text{Cv}[X]$  with (Coles, 2001, Section 2.2, Upton and Cook, 2008)

$$E[X] = \int_{-\infty}^{\infty} xf(x)dx = \int_1^0 x d\bar{F}(x), \text{Var}[X] = \int_1^0 (x - E[X])^2 d\bar{F}(x), \text{Sd}[X] = \sqrt{\text{Var}[X]}, \text{Cv} = \frac{\text{Sd}[X]}{E[X]} \quad (12)$$

According to (12), any scaling of  $X$  by a factor  $S > 0$  results in proportional scaling of expectation and standard deviation in (12), and the CV remains constant. Correspondingly, random magnitude  $s$  in (9,10) only scales the field  $s_x(x)$  in the max-stable case with  $\beta = 0$  and influences the expectation of  $A(z)$  but not the CV. Thus, the CV is independent on the expectation. This does not apply to the non-max-stable case with  $\beta \neq 0$  in (9,10). These different behaviors are detectable for the examples of Figure 1 b and d in Figure 3 c and d. For the max-stable case, the scale/slope parameter of the linearized regression function does not differ significantly from 0 according to the t-test (Fahrmeir et al., 2013, Section 3.3). For max-stable case, the

regression function is statistically significant with a p-value of 0.00. Linearization is provided by logarithm of CV and expectation/average. For completeness, the full dependence case of Figure 3 b corresponds with an CV 0.

In sum of Section 2, Schlather's 1<sup>st</sup> Theorem has parallels to NatCat models, is used already in hazard models and was extended here to the non-max stable case regarding spatial dependence and characteristic. Statistical indication for max-stability is the independence of the spatial dependence measure from the block size (e.g., one versus ten years) and independence between CV and expectation of the area function (11). Otherwise, non-max-stability is indicated.

275

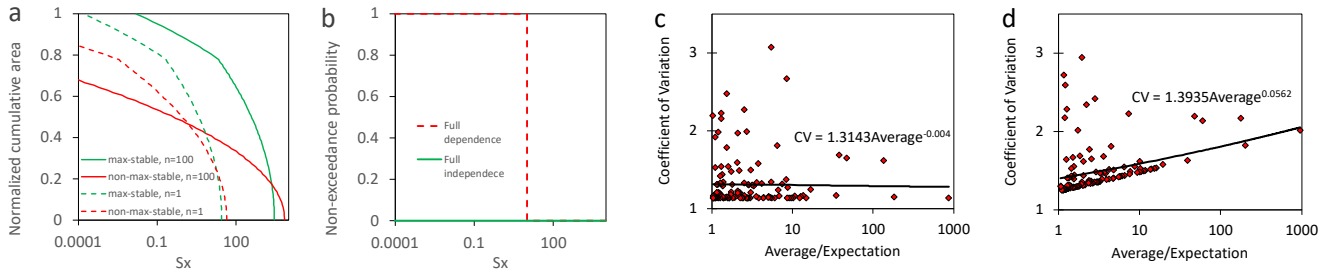


**Figure 3: The area function and corresponding characteristics: a) area function of the biggest event of Figure 1, b) area functions for the limit cases (examples), c) relation CV to average for max-stable case of Figure 1 b, d) for non max stable case of Figure 1 d (events with average >1, distance between the support points is 0.1 for the computation of the average in region (-4,4)).**

280

### 3 The combined return period (CRP)

#### 3.1 The stochastic derivation

Let the point event  $s_{x,i}$  be the local intensity at site  $x$  of a hazard event  $i$  as a member of the set of all events of a defined unit period such as a year, hazard season, or half season. This local event intensity might be the maximum river discharge of a flood, the peak ground acceleration of an earthquake or the maximum wind gust of a windstorm event. The entire number of events with  $s_{x,i} > z$  during the unit period is  $K = \sum_{i=1}^{\infty} \mathbf{1}(s_{x,i} > z)$ .  $K$  is (at least approximately) a Poisson distributed (Upton and Cook, 2008) discrete random variable with an expectation - the expected exceedance frequency, that is the local hazard function in a NatCat model (this is not the hazard function/hazard rate of statistical survival analysis, Upton and Cook, 2008).

285

$$\Lambda(z) = E[K]. \tag{13}$$

This is the bjective frequency function. The and the local hazard curve. Its reciprocal of expected local EF is determines the local hazard curve for the RP

290

$$T(x) = 1/\Lambda(x).$$

295

$$T(z) = \frac{1}{\Lambda(z)} = \frac{1}{E[K]}. \tag{14}$$

As  $X_{s_x}$  is a point event it's RP  $T(s_x)$  is also a point event and the EF of a point process with frequency function of  $T$  is according to (14)

$$A(\lambda \Lambda_T(z)) = 1/\lambda. \tag{15}$$

It might be called the RP process. In the Supplementary (Figure 1), the EF function is depicted beside realizations, one of a single process and a second of two associated processes. In extreme value theory and statistics (Coles, 2001; Beirlant et al., 2004; Falk et al. 2011), the density of point events  $T$  at the line of positive real numbers is expressed by the Poisson process's intensity, being the negative first derivative of (3).

Two point processes can be associated. Since (15) is the same as (8), Schlather's theorem and our extensions directly apply to RP. For completeness, the marginal maxima have a CDF for  $n$  unit periods (a unit Fréchet distribution for  $n = 1$  according to (3))

$$G_n(z) = \exp(-n\Lambda_T(z)) = \exp(-n/z). \tag{16}$$

This is applicable because the probability of non-exceedance for level  $z$  of the block maxima is the same probability that no events occur with  $s_{x,i} > z$  which is determined by the Poisson distribution; (6,8) also imply this link.

Schlather's theorem is also based on and implies the concept of pseudo polar coordinates. According to de Haan (1984;) and well explained by Coles (2001) and Falk et al. (2011, Section 8.3.2), two max-stable linked point processes with expected exceedance frequency (15) and point events  $T_1$  and  $T_2$  are also represented by pseudo polar coordinates with radius  $R$  and angle  $V$

$$R = T_1 + T_2, V = \frac{T_1}{T_1 + T_2}, \text{ corresponding } T_1 = RV, T_2 = R(1 - V) = T_1 \frac{1-V}{V}. \tag{17}$$

$$\left\{ R = T_1 + T_2, V = \frac{T_1}{T_1 + T_2} \right\} \Leftrightarrow \left\{ T_1 = RV, T_2 = R(1 - V) = T_1 \frac{1-V}{V} \right\}. \tag{18}$$

As we describe in the Supplementary, Section 1, the expectation of the random element  $(1 - V)/V$  is 1 and for the conditional expectation of unknown RP  $T_2$  with known  $T_1$  applies (association is provided)

$$E[T_2|T_1] = T_1. \tag{19}$$

The interest in extreme value theory and statistics (Coles, 2001, Section 3.8; Beirlant et al., 2004, Section 8.2.3; Falk et al. 2011, Section 4.2) is focused on the distribution function of pseudo angle  $V$  with cumulative distribution function (CDF)  $H(\lambda)$ .

It determines the dependence structure, called copula (Marie and Kotz, 2001), of the block maxima of the  $z$ . As Coles (2001) write “the angular spread of points of  $N$  [the entire point processes—here local maxima of all point events  $T$  (or  $X$ ) during  $k$  considered unit periods (e.g., half years, a season, years, or decades). The univariate CDF of maximum occurred RP of  $k$  unit periods considers  $A(x)$  of (1) and also of (3)

$$G_k(x) = \exp(-kA(x)) = \exp(-k/x).$$

(6)

If the copula of a bivariate distribution  $G_k(x_1, x_2)$  of two local maxima is max-stable, the dependence between annual maxima determined by  $H$ , and is the same as between century maxima. It is also called extreme value copula (Marie and Kotz, 2001). The independence gives this max stability of the dependence structure between pseudo-independent of radial distance  $[R]$ , angle  $\psi$  and pseudo-radius  $R$  occurs independently to each other and  $H$  determine the copula between two marginal maxima  $Z(x)$  in (4) (Theorem 1.

According to Coles, (2001). The occurrence of, Section 3.8), the pseudo radius  $R$  in (17) is once again a point event of a Poisson process with EF frequency  $\Lambda(x) = 2/x$  - the double of (315). This means the average of two RP  $T_1$  and  $T_2$  results in a combined return period (CRP)  $T_c$

$$T_c = \frac{T_1 + T_2}{2},$$

(19)

with EF exceedance frequency function (3). This 8,15). We do not have a mathematical proof that (18,19) also applies for the non-max-stable associated point processes. However, max-stable case between and non-max-stable cases have the same limits - full dependence ( $T_1 = T_2$ ) and no dependence/full independence ( $T_1 = 0$  if  $T_2 > 0$  and vice versa,  $T_1 = T_2 = 0$  represents the lack of a local event). These are also the limits of non max stable dependence structures. Therefore, CRP (19) should also apply for the non-max-stable dependence, which case between these limits. This can be validated heuristically as shown we demonstrate by an example in the Supplementary. The critical result is that the average of two RPs is again an RP with EF (Section 3). Such reproductivity does not apply to a metric of the EF or the logarithm of RP. RP has probably been

More than one RP can be averaged in NatCat studies before, but it was not known that this average remains an RP since the averaging of two RPs can be done in serial (and the pseudo polar coordinates are also applied to more than two marginal processes). Serial averaging (averaging the last result with a further RP) also implies a weighting; the first considered RPs would be smaller weighted than the last in the final CRP. The general formulation of averaging of RP with weight  $w$  is

$$T_c = \frac{\sum_{j=1}^n T_j w_j}{\sum_{j=1}^n w_j}.$$

360

$$\left( \frac{\sum_{i=1}^n T_i w_i}{\sum_{i=1}^n w_i} \right)$$

(20)

The corresponding continuous version via a defined region in a geographical within the region's bounds  $u$  and  $l$  in space with coordinates  $z$  is  $\mathbb{R}^d$

365

$$T_c = \frac{\int_{\text{region}} T(z)w(z)dz}{\int_{\text{region}} w(z)dz}$$

(8)

$$\text{For weight } T_c = \frac{\int_l^u T(x)w(x)dx}{\int_l^u w(x)dx} \tag{21}$$

370

If  $w(z) = (x) = 1$ , the integral applies in (21) then the denominator is the area of the region- and CRP  $T_c$  is the expectation of the area function (11). This also applies for other weightings if we consider it in the area function, here written for RP  $T(x)$

## **2.2 Opportunities and implications**

$$A(z) = \frac{\int_l^u w(x)1(T(x) \geq z)dx}{\int_l^u w(x)dx} \tag{22}$$

with empirical version for  $n$  measuring station  $i$  in the analyzed region

375

$$A(z) = \frac{\sum_{i=1}^n w_i 1(T_i \geq z)}{\sum_{i=1}^n w_i} \tag{23}$$

The weighting, especially the empirical one, can be used in hazard research to compensate an inhomogeneous geographical distribution of measurement stations or a different focus than the covered geographical area such as the inhomogeneous distribution of exposed values or facilities in NatCat research. It has the same effect on the area function as a distortion of the geographical space as used by Papalexioiu et al. (2021). Weighted or not, CRP and CV are parameters of the area function.

380

## **3.2 Testability**

Before the CRP is applied in stochastic NatCat modelling, it should be tested statistically to validate the appropriateness. A sample of CRPs can be tested by a comparison of its EF exceedance frequency function (315) and their empirical variant. Therein the empirical EF of the largest CRP in the sample is the reciprocal of the length of the observation period. The 2<sup>nd</sup> largest CRP is hence associated to twice the EF exceedance frequency of the largest CRP and so on. It is the same as for empirical exceedance frequency for EQ (e.g., the well-known Gutenberg -Richter relation in Seismology, Gutenberg-Richter, 1956). However, not all small events are recorded; the sample is thinned and incomplete in this range. This is. This completeness issue is well known for earthquakes and is here less important if only the distribution (616) of maximum CRPs

385

are tested. There are a number goodness-of-fit tests (Stephens, 1986, Section 4.4) for this situation with the case of known distribution model. The Kolmogorov-Smirnov test is a popular variant.

390 **Besides that, 3.2 The scaling opportunity**

The CRP also offers the opportunity of stochastic scaling. The CRP  $T_c$  and all  $n$ -local RPs  $T_i$  in (7) or (20) (and  $T(z)$  in (8), and by this, the pseudo radius  $R$  in (4) or (21)) are scaled via a factor  $S$ . The pseudo angle  $V$  stays the same:

$$T_{cs} = T_c S, \quad T_s(z) = T(z) S, \quad T_{s,j} = T_j T_{s,i} = T_i S, \quad (24)$$

This means for the pseudo polar coordinates in (17), which applies to the max-stable case,

395  $R_s = R S, \quad V_s = V.$

$$SR, V_s = \frac{T_{s,1}}{T_{s,1} + T_{s,2}} = \frac{ST_1}{S(T_1 + T_2)} = V. \quad (25)$$

400 The pseudo angle  $V$  is not changed as expected since pseudo radius and pseudo angle are independent in the pseudo polar coordinate for the max-stable case (Section 3.1). This also means that a scaling must be more complex if there is non-max-stability. We cannot offer a general scaling method for this situation; however, it must consider/reproduce the pattern of the relation CV versus CRP (example in Figure 3 d) adequately. Irrespective of this, the corresponding event field of local intensities (e.g., maximum wind gust speed) can be computed for the scaled RPs via the inverse of the EF function (1) of local intensity. If the association between the local point processes is max-stable, the value of  $H(V)$  is not changed, and nothing is changed in the sampling regarding dependence. This matches the scaling in Schlatter's (2002) two theorems about max-stable random fields (by Schlatter's random element  $s$ ). Such simple scalability does not apply if we lack max-stability in the spatial dependence; an extensive scaling without special considerations would be critical because of uncontrolled consequences. local RPs via the inverse of the local hazard function  $T(z)$  in (14) or  $A(z)$  in (13).

**3.4 Risk estimates by scaling and averaging**

410 The main goal of a NatCat risk analysis is the estimate of a risk curve (Mitchell-Wallace et al., 2017, Section 1), the bijective functional of event loss in a region and corresponding RP, called here event loss return period (ELRP)  $T_E$ . As aforementioned, there are two approaches for such estimates with corresponding pros and cons. We introduce an alternative method. According to (18), the expectation of an unknown ELRP  $T_E$  is the CRP  $T_c$  of the local event intensities; the CRP is an estimate of the ELRP (max-stability between ELRP and CRP provided). To get a good estimate of ELRP, we must average the  $T_c$  of many events with the same event loss. We cannot observe such, but we can stochastically scale historical events respectively their local intensity observations. The modelled event loss  $L_E$  is the sum of the product of local loss ratio  $L_R$ , determined by local event intensity  $s_{x,i}$  and local exposure value  $E_i$  over all sites  $i$  (Klawa and Ulbrich, 2003; Della-Marta et al. 2010)

$$L_E = \sum_{i=1}^n L_{R,i}(s_{x,i})E_i \quad (26)$$

with the local vulnerability function  $L_{R,i}(s_{x,i})$ . To get the event loss for the scaled event, the observed  $s_{x,i}$  is replaced by

$$s_{xs,i} = A_i^{-1} \left( \frac{A_i(s_{x,i})}{S} \right) \quad (27)$$

with local hazard function  $A(z)$  (13) for exceedance frequency and its inverse function  $A^{-1}(z)$ . The formulation with RP (14) is equivalent. The scaling factor  $S$  in (27) is the same for all sites/locations  $i$  respectively as it is in (24) for the CRP and must be adjusted in an iteration until the defined event loss is the result of (26). The scheme in Figure 4 a includes all elements and relations of the scaling approach. Therein, the numerical determination in the scaling scheme has only one direction, from scaled CRP to the event loss. The idea of CRP averaging is also illustrated by Figure 4 b. The standard error of the averaging is the same as for the estimates of an expectation by the sample mean (Upton and Cook, 2008, catchword central limit theorem).

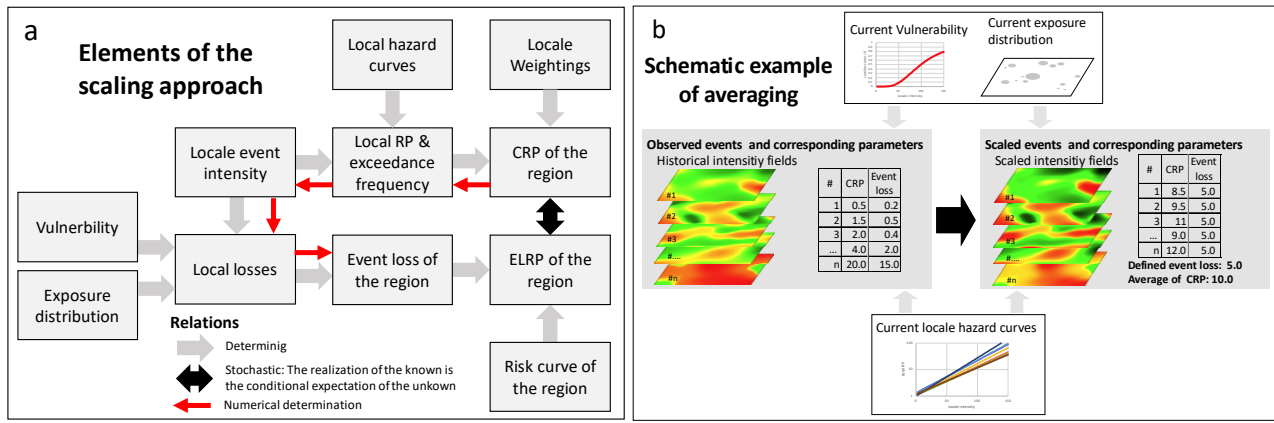


**Figure 4: Schemes of the scaling approach: a) elements and relations, b) schematic example for estimation of event loss by averaging of CRP.**

According to the well-known Delta method, well explained by Coles (2001, Section 2.6.4), statistical estimates and their standard error can be transferred in other parameter estimation and corresponding standard error by the determined transfer function and its derivatives. In its meaning, we can also average the event loss for a fixed/determined CRP respectively its scaled variant. This also applies to the exceedance frequency, the reciprocal of RP, for a determined/fixed event loss.

There is a further chain of thoughts as argument for averaging the exceedance frequency. The scaled intensity fields are like sub-sets in the set of all possible event fields. Each of these subsets implies a relation exceedance frequency to event loss – a risk curve. Furthermore, we assume an unknown probability that this sub-set generates a part of the entire risk curve. The latter is for a fixed event loss the aggregation of subset exceedance frequency multiplied with their probability. This is basically the same as the definition of the expectation (12). Therefore, we can apply estimator of the expectation in the estimation of a risk curve and average the exceedance frequencies of risk curves of the subsets – the scaled event fields.

All mentioned estimators for risk curve via scaling and averaging over  $n$  events are

$$\hat{T}_E(L_E) = \frac{1}{n} \sum_{i=1}^n T_{CS,i}(L_E), \hat{\Lambda}_E(L_E) = \frac{1}{n} \sum_{i=1}^n 1/T_{CS,i}(L_E), \hat{L}_E(T_E) = \frac{1}{n} \sum_{i=1}^n L_{E,i}(T_{CS} = T_E). \quad (A)$$

further opportunity is to present all local RPs of an event in a defined region via Raschke's (2013) cumulative area function, which is normalized here to provide comparability.

$$A(x) = \frac{\int_x^{\infty} w(z)I(T(z))dz}{\int_x^{\infty} w(z)dz}, I(T(z)) = 1 \text{ if } T(z) \geq x, \text{ otherwise } I(T(z)) = 0. \quad (10)$$

445

Jung and Schindler (2019) have recently published a similar cumulative presentation for local wind speed maxima of storm events. The function  $A(x)$  is like the survival function of a (conditional) random variable, here the local RPs of the event. The CRP  $T_E$  represents the expectation (or its estimate). It can also be derived from the moments of random variables that the coefficient of variation (CV; Upton and Cook, 2008) for (10) is not be concerned about scaling (9) for max-stable situations. This implies that the CV is independent of CRP in the case of max-stability. This underlines that the CRP and area function corresponds with maxima's spatial dependence in the sense of max-stable random fields (Schlather, 2002).

450

### 2.3 Analysis of (28)

The right side of the equations in (28) implies actual values which can be and are replaced by estimates. Corresponding uncertainties must be considered in the final error quantification.

455

We draw attention to the fact that the explained scaling does not change the CV of (23) which implies independence between CRP and CV (Section 2.4). Therefore, the presented scaling only applies to the max-stable case of local hazard. For the non-max-stable case, the scaling factor  $S$  in (27) must be replaced event wise by  $S_i$  which reproduce the observed relation between CRP and CV. An example without max-stability was shown in Figure 3 d.

## **4 Application to German winter storms**

460

### **4.1 Overview about data and analysis**

We have selected the peril winter storms (also called extratropical cyclones or wind winter windstorms) over Germany to demonstrate the application of CRP, we analyze opportunities of the CRP because of good data access and since we are familiar with this peril (Raschke et al., 2011; Raschke, 2015). Our analysis follows the scheme in Figure 4 a, important results are presented in the subsequent Sections, technical details are explained in Section 5. At first, we give an overview.

465

We analyzed 57 winter storms (also called winter windstorms) over Germany over 20 years, from autumn 1999 to spring 2019. Wind station data have been provided by the German meteorological service (DWD, 2020). Different completeness criteria were considered for station selection, and (Supplementary Data, Table 1 and 2) to validate the CRP approach. Different references (Klawa and Ulbrich, 2003; Gesamtverband Deutscher Versicherer, [GDV], 2019; Deutsche Rück, 2020) have been considered for selecting to select the time window per event. The lists are presented in the Supplementary (Excel file). The one and Our definition of a half power of wind speed maximum are analyzed as local peril intensity. The reason winter storm

470



season is explained in Section 3.1 and the appropriateness of the Gumbel distribution for the from September to April of the subsequent year and accept a certain opportunity of contamination of the sample of block maxima of local event intensities and corresponding computation of RP per event with bias correction. To increase the accuracy of estimates by higher extremes from convective windstorm events and a certain opportunity of incompleteness since extratropical cyclones can also be observed outside our season definition (Deutsche Rück, 2020). The term winter storm is only based on the high frequency of extratropical cyclones during the winter. The seasonal maximum is also the annual maximum of this peril.

The maxima per half season (bisected by turn of the year) are analyzed to double the sample size and to increase estimation precision. The appropriateness of this sampling is discussed in Section 5.1. We considered records of wind stations in Germany of DWD (2020; *FX MN003*, a daily maximum of wind peaks [m/s], usually wind gust speed) that include minimum record completeness of 90% for analyzed storms, at least 90% completeness for the entire observation period and minimum 55% completeness per half season. Therefore, we analyze the maxima of half seasons per only consider 141 of 338 DWD wind stations (Supplementary Data, Table 3). We think this is a good balance between large sample size and high level of record completeness.

The intensity field per event is represented by the maximum wind gust for the corresponding time window of the event at each considered wind station. The local RP per event is computed by a hazard model per wind station. This is an implicit part of the estimated extreme value distribution per station as explained in Section 5.1. The resulting CRPs per event and corresponding statistical tests are presented in the following Section 4.2. We have considered two weightings per station, capital, and area. Both are also computed per wind station by assigning the grid cells with capital data of the Global Assessment Report (GAR data; UNISDR, 2015) via the smallest distance to a wind station. We also use this capital data to spatially distribute our assumed total insured sum 15.23 Trillion € for property exposure (residential building, content, commercial, industrial, agriculture and business interruption) in Germany in 2018. This is based on Waisman's (2015) assumption for property insurance in Germany and is scaled to exposure year 2018 under consideration of inflation in building industry (Statistisches Bundesamt, 2020) and increasing building stock according to the German insurance union (GDV, 2020). It is confirmed by the assumptions of the Perils AG (2021), however their data product is not public. We also used loss data of the GDV (2019) for property insurance, when we fitted the vulnerability parameters for the NatCat model. These event loss data of 16 storm during a period of 17 years are already scaled by GDV to exposure year 2018.

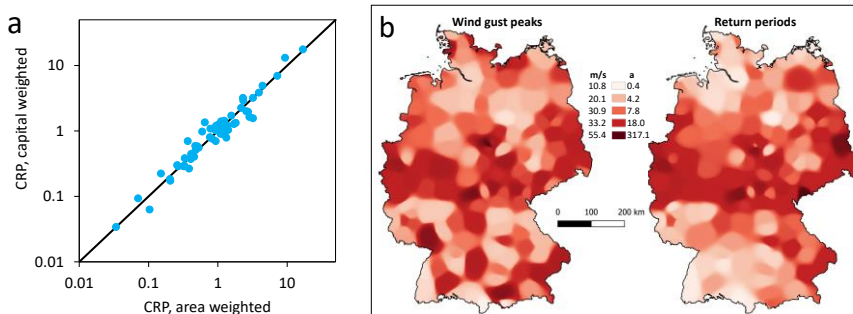
The spatial characteristic is analyzed in Section 4.3 according to the aspects of Section 2.4 with focus on the question if there is max-stability or not in spatial dependence and characteristic. Finally, we present the estimated the risk curve for the portfolio of the German insurance market in Section 4.4 including a comparison with previous estimates. Details of the vulnerability model are documented in Section 5.2. The concrete numerical steps, the applied methods to quantify the standard error of estimates, and the consideration of the results from vendor models are explained in Section 5.3, 5.4 and 5.5.

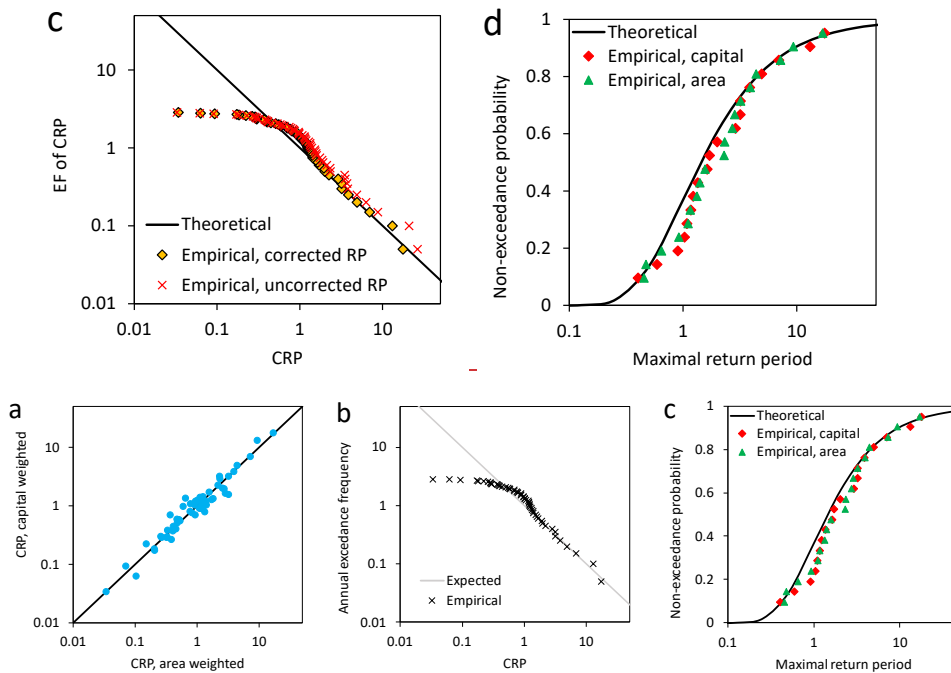
## 4.2 The CRP of past events and validation

As announced, we have computed the CRP according to (20) with the wind gust peaks listed in the Supplementary. We considered simplified area weights and the grid's capital weights from Global Assessment Report (GAR; UNISDR, 2015), assigned to the wind station by shortest distance. The first variant considers the storm as a pure phenomenon in the geographical space; the second is more focused on consequences. The Data, Table 2, and local hazard models according to (30). Our local hazard models are discussed in Section 5.1 and parameters are presented in the Supplementary Data, Table 4. We have considered two weightings for the CRP, a simple area weighting and a capital weighting (Supplementary Data, Table 3). In Figure 5 a, we compare the estimates which do not differ so much; the approach is robust in the example. The most significant winter storm of the observation period is Kyrill (that occurred in 2007). It has CRPs of  $16.97 \pm 1.75$  and  $17.64 \pm 1.81$  years (area and capital). Both are around in the middle of the estimated range 15 to 20 years by Donat et al. (2011). CRPs Further estimates are compared listed in Supplementary Data, Table 1.

In Figure 5-a for a one year unit period (equal to one season). For example, the simply interpolated event fields (one is the wind field) for Kyrill are shown in Figure 1 b. In Figure 1 d and e b, the results are validated according to Section 3.2. The empirical EF exceedance frequency matches well with the theoretical one for  $T_c \geq 1.65$ . Small CRPs are affected by the incompleteness of records: our record list. In the medium range, the differences between the model and empiricism are not statistically significant (for. In detail, we observe 27 storms with  $T_c \geq 1$  within 20 years; expected were 20. According to the Poisson distribution the probability of 7.8% for the 27 exceedances or more for 20 years). The bias correction of local RP affects higher CRPs (is 7.8%. A two-sided test with  $\alpha = 5\%$  would reject the model if this exceedance probability would be 2.5% or smaller.

The seasonal/annual maxima of CRP must follow a uniform Fréchet distribution ( $\alpha = 1$  in (3)) according to (16). We plot this and the empirical distribution in Figure 5 c). In Figure 1 d, the maximum CRP of a season follows the CDF (6) very well. The Kolmogorov-Smirnov (KS) test (Stephens, 1986, Section 4.4) for the fully specified distribution model accepts the our model for at the extremely high significance level of 25% (the pure KS statistic is 0.1422, sample size  $n = 20$ ) for the capital weighted variant. Usually, only level 5% is used; however, the KS test considered. This result should not be affected seriously by the absence of one (probably the smallest) maximum due to an incomplete event list incompleteness issue. In summary, we state that the CRP offers a stable, testable, and robust method, to stochastically quantify winter storms over Germany.





530

**Figure 5: Results of the analysis: a) comparison of area and capital weighted CRPs, b) Storm Kyrill, 2007, inverse distance weighting (by software Qgis with distance parameter 6) for local wind peaks as reproduction of the wind field and field of local RP (same colour — same percentile), c) comparison of theoretical and observed EF of CRPs with influence of correction, d) CRP, c) test of distribution of seasonal maxima of CRP with capital weighting of a seasons (equivalent with annual maxima).**

535

As aforementioned, the CRP corresponds with the dependence between local RPs. Therefore, the characteristic of spatial dependence between block maxima is also analyzed. The plot of the estimates of dependence measure Kendall's  $\tau$  (Upton and Cook, 2008) is depicted in Figure 2 b. It decreases by increasing distance. The scatter range of the half seasons is smaller than for two seasons due to different sample sizes. In Figure 2 c, we also compare Germany with results for Switzerland (Raschke et al., 2011). For the latter, the spatial dependence is smaller, probably because of the alpine topography. The sample mean of Kendall's  $\tau$  decreases by value 0.05 with increasing block size (half season versus two seasons). This is statistically significant; the normally distributed confidence range of estimated expectation of the differences indicates probability 0.002 for values  $\leq 0$ . Max stability is unlikely. The characteristics of spatial dependence also influence the area functions in Figure 2 e. The hypothetical case of fully spatial dependence is shown as a benchmark (CRP 100 years) and has no scattering with a CV of 0. The scaling opportunity is demonstrated by the storm Kyrill of 2007 with  $T_{es} = 100$  years. The differences between area functions of the area and capital weightings depend on the concrete storm. The CV should be independent of RP in case of max stable dependence. This does not apply according to Figure 2 d; it increases by increasing CRP in the regression model for capital weighted CRP. The  $p$  value is 0.002 for an exponent  $\leq 0$ ; this confirms the non max stable behavior of Kendall's  $\tau$ . The estimates of the exponent differ insignificantly (area versus capital weighting). Details of our more complicated proxy for

540

545

550 non-max-stable scaling are presented in Supplementary. In Figure 2c, the relation between scaled CRP and CV of the proxy is shown. The regression function of Figure 2 d is reproduced.

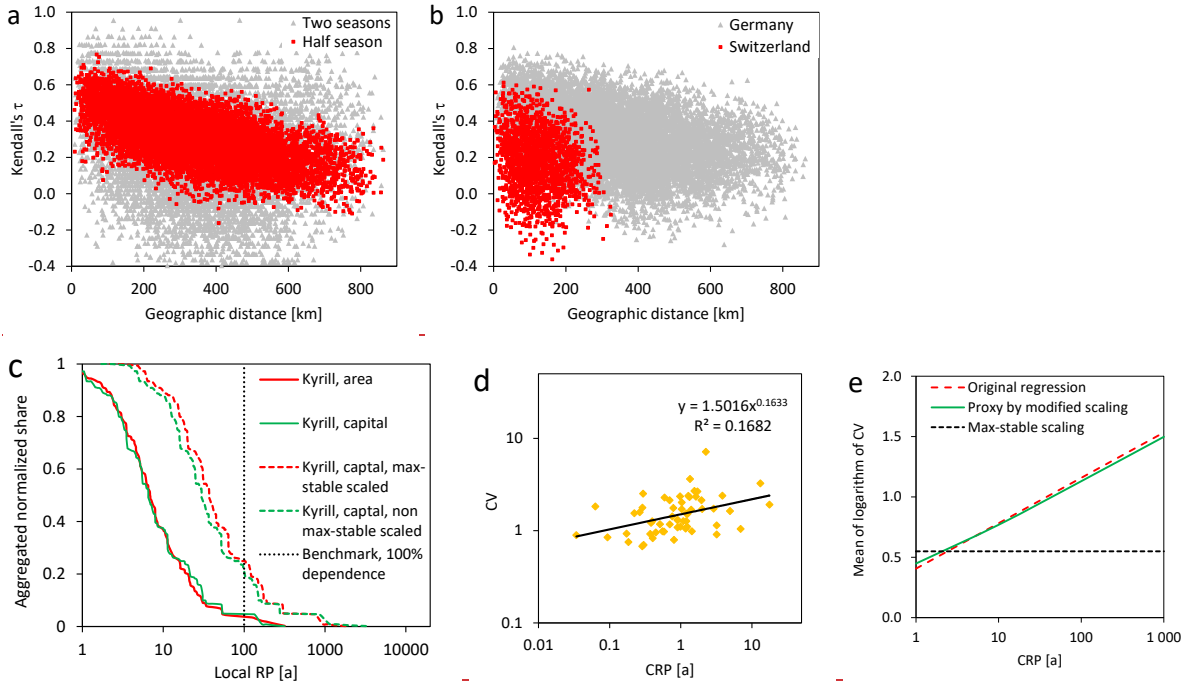


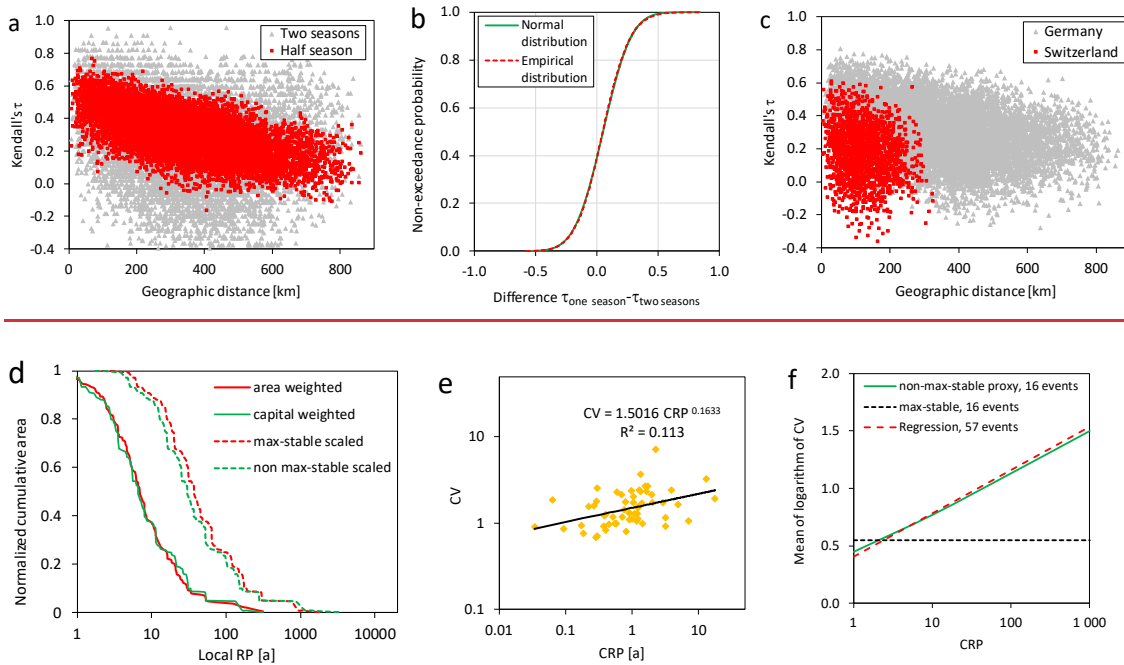
**Figure 2: Spatial characteristics: a) 4.3 Spatial characteristic and dependence**

555 As discussed in Section 2.4, the spatial characteristic is an important aspect from stochastic perspective. Therefore, we have analyzed the relation between distance and dependence measure. Here we have applied Kendall's  $\tau$  (Kendall, 1938; Mari and Kotz, 2001, Section 6.2.6) and show the dependence between half-season maxima and two season maxima for 9,870 pairs of stations in Figure 6 a. Since the sample sizes is relatively small, the spreading is strong that is caused by estimation error. Furthermore, the differences between the estimates for one hazard season maxima and two hazard seasons maxima are almost perfectly normal distributed and should be centered to 0 in case of max-stability (CDF in Figure 6 b). This does not apply with expectation 0.051 and standard deviation 0.182. According to a normally distributed confidence range for the estimated expectation with standard deviation 0.002, the probability, that the actual value is  $<0$ , is smaller than 0.00. This is in line with the differences of the non-max-stable example in Figure 2 b.

560 For completeness, we compare the current estimates of Kendall's  $\tau$  with these for Switzerland from Raschke et al. (2011) in Figure 6 c. The spatial dependence is higher for Germany. A reason might be differences in the topology.

565 We have also computed the area functions and show examples in Figure 6 d for winter storm Kyrill. The different weightings result in similar area functions. The CRP and CV of all events are plotted in Figure 6 e. The regression analysis result in statistical dependence between CRP and CV. For the linearized regression function, the p-value is 0.002 (t-test, Fahrmeir et al., 2013, Section 3.3). Because two statistical indications of non-max-stability, we develop for every event a local

570 scaling that consider the global scaling factor and the ratio between local RP and CRP. In this way, we could reproduce the observed pattern (Figure 6 f). Details of this workaround are presented in the Supplementary, Section 7. The differences between the scaling variants for storm Kyrill do not seem to be strong (Figure 6 d).



575 **Figure 6: Spatial characteristics of winter storms over Germany: a) estimated Kendall's  $\tau$  versus distance, b) differences between Kendall's  $\tau$  for different block sizes, Germany, b) estimated Kendall's  $\tau$  versus distance for a season-forseasonal maxima in Germany and Switzerland (Raschke et al., 2011), c) estimated Kendall's  $\tau$  versus distance for a season-forseasonal maxima in Germany and Switzerland (Raschke et al., 2011), d) area functions, and d) for storm Kyrill with scaling to CRP 100 years, e) relation CV of local RP versus CRP (of capital weighted), area functions, and e) approximation of this relation by modified, non-max-stable special stochastic scaling.**

580 **2.4.4 The risk estimates by averaging**

The interest of NatCat risk analysis is in the risk curve, i.e., the relation between an event loss  $L_E$  and its RP  $T_E$ . It is a bijective. Before we estimated risk curves according to the approach of Section 3.4, we must estimate a vulnerability function  $L_E(T_E)$  with its inverse variant  $T_E(L_E)$  and can be estimated by relation (5) and our concept of scaled CRP. The latter implies a (modelled) event loss  $L_E$  for the scaled field of local RP (9) and corresponding local intensities (catchword local hazard curve). The local intensity, vulnerability and exposure value determine the local (expected) loss. Its aggregation over the geographical space (31) which determines the event losses  $L_E$  with RP  $T_{ES}$ . The stochastic link between  $T_{ES}$  and  $T_E$  is (5), and the risk curve can be estimated by variants of averaged metrics of  $n$ -scaled historical wind fields respectively corresponding wind records

590  $\hat{T}_E(L_E) = \frac{1}{n} \sum_{i=1}^n T_{CS,i}(L_E), \hat{\Lambda}_E(L_E) = \frac{1}{n} \sum_{i=1}^n 1/T_{CS,i}(L_E), \hat{L}_E$  local loss ratio  $L_R$  in the event loss aggregation (26). We fit  
the scaling parameter on the event loss  $(T_E) = \frac{1}{n} \sum_{i=1}^n L_{E,i}(T_{CS} = T_E)$ . (14)

Further details of the concept are explained and illustrated in Section 4.  
Our demonstration object remains Germany, and we estimate its risk curve for insured winter storm losses. The local losses are simply the product of local exposure value and loss ratio  $L_R$ . This is determined by local maximum wind speed per event via the (local) vulnerability function (loss or damage function). Our loss function follows the approach of Kława and Ulbrich (2003) and is fitted by the data of the General Association of German Insurer (GDV, 2019) for 16 historical events from 2002 to 2018 (Figure 3 a). These loss data are already inflated/scaled to the German insurance market 2018. An exemplary variant of our vulnerability functions is compared to previous models in Figure 3 b; different geographical resolutions might explain the differences. The processed model of the geographical distribution of exposed values is the same as for capital weighting in the previous section. The assumed total sum insured (as plotted in Figure 7 a. The details of the vulnerability function and its parameter fit are explained in Section 5.2. Then, we use the vulnerability function in the three variants of risk curve estimates of Section 3.4 – averaging of event loss, ELRP or its reciprocal, the exceedance frequency. Details of the numerical procedure are explained in Section 5.3 which corresponds with the scheme in Figure 4a.

600 In Figure 7 b, the three estimated risk curves according to the three estimators in (28) are presented for max-stable scaling and differ less to each other what indicates the robustness of our approach. The empiricism is presented by the historical event losses and their empirical RP (observation period 17 years of GDV loss data) and capital weighted CRP. In addition, we present the range of two standard errors of the estimates of loss averaging which implies the simplest numerical procedure. Details of uncertainty quantification are explained in Section 5.4.

605 The differences between max-stable and non-max-stable scaling in the risk estimates are demonstrated in Figure 7 c. For smaller RP, no significant difference can be stated in contrast to higher RP. This corresponds with the differences between the CV in relation to the CRP for max-stable and non-max-stable case in Figure 6 f. These are also higher for higher CRP.

We also compare our results with previous estimates in Figure 7 c. For this purpose, we must scale these to provide comparability as good as possible. The relative risk curve of Donat et al. (2011) is scaled simply by our TSI is 15.23 Trillion euros and based on the assumptions of assumption for exposure year 2018. The vendor models of Waisman (2015) are scaled by the average of ratios between modelled and observed event losses from storm Kyrill since a scaling via TSI for Germany is scaled/inflated from 2015 to 2018 by factor 1.12 under consideration of increasing construction prices (Statistisches Bundesamt, 2020) and building stock (GDV, 2019).

615 The three risk curves, that have been estimated by (9) with wind fields scaled by capital weighted CRP are shown in Figure 3 c. Also, reported losses of historical events<sup>9</sup> and their empirical RP (observation period of 17 years) and the estimated CRP are plotted. The differences between the risk curves are minor. The standard error (SE) of estimates by loss averaging (also called RP scaling) is more minor than 8.5% of the estimated event loss for RP  $T_E \leq 400$  years. The range of two SE is not a confidence range for empirical RP. Its uncertainty is higher and explains the higher differences to the risk curves.

Since German winter storms do not imply max-stable dependence, we also estimate the risk by non-max-stable scaling. The result is depicted in Figure 3 d and shows lower event losses for high RP than in the max-stable case. We also compare our risk curves with these vendor models, which have been presented by Waisman (2015). However, the exposure assumptions are not the same (exposure year, was not possible (uncertain market share, and split between residential, commercial, and industry). To provide comparability, the vendor estimates are scaled by factor 1.34. This is the average of the ratios between reported and modeled loss for storm Kyrill. We also consider the risk estimate by Donat et al. (2011) and exposure). The result of the standard model of European Union (EU) regulations (European Commission, 2014), also known as Solvency II requirements. It considers the exposure per CRESTA zone (, is also based on our TSI assumption, split into the Cresta zones by the GAR data. The Cresta zones ([www.cresta.org](http://www.cresta.org)). For the standard model, we split our assumed TSI to the Cresta zones by the GAR data. The same TSI is used to scale Donat's et al. (2011) estimated RP for event loss ratios (NCEP variant in Figure 7); our extrapolation complies with their distribution assumption. We highlight that we cannot fully ensure comparability to the previous risk estimates) are an international standard in insurance industry and corresponds to the two digit postcode zones in Germany.

The risk estimate of Donat et al. (2011) is based on a combination of frequency estimation and event loss distribution by the generalized Pareto distribution which is fitted on a sample of modelled event losses for historical storms. The corresponding risk curve differs very much from other estimates and obviously overestimate the risk of winter storms over Germany. The standard model of EU only estimates the maximum event loss for RP 200 years, the estimated event loss is very high. The vendor models vary but have a similar course as our risk curves. The non-max-stable scaling is in the lower range of the vendor models, the unrealistic max-stable scaling is more in the middle. The concrete names of the vendors can be found in Waisman's (2015) publication. The reader should be aware that the vendors might have updated their winter storm model for Germany in the meantime.

The major result of Section 5 is the successfully demonstration that the CRP can be applied to estimate reasonable risk curves under controlled stochastic conditions. We have also discovered the high influence of the underlying dependence model (max-stable or not) and corresponding spatial characteristic to loss estimates for higher ELRP.

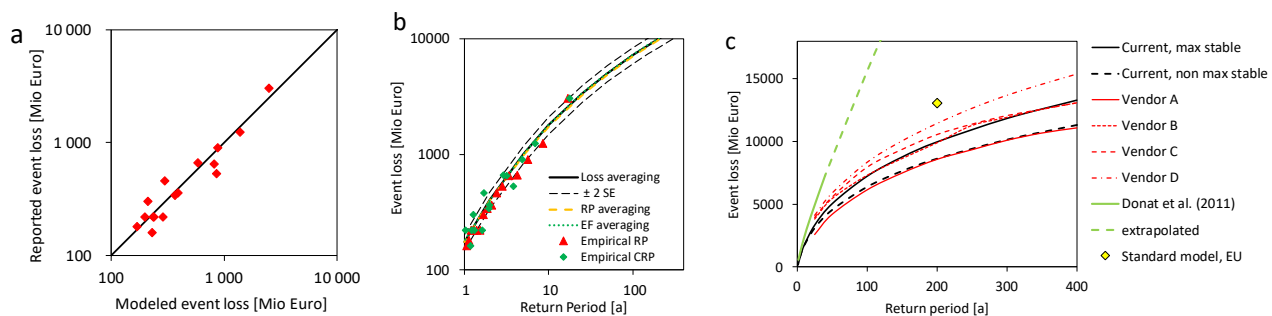


**Figure 7: Estimates for insured losses from winter storms in Germany: a) reported versus modelled event losses, b) current risk curves and observations, c) influence max-stable and non-max-stable scaling and comparison to scaled, previous estimates (Donat et al., 2011; Waisman, 2015, European commission, 2014).**

## 5 Technical details of the application example

### 5.1 Modelling and estimation of local hazard

As aforementioned, the maximum wind gusts of half seasons of winter storms (extratropical cyclones), the block maxima, have been analyzed. Therein the generalized extreme value distribution (Beirlant, et al., 2004, (5.1)) is applied

$$G(x) = \begin{cases} \exp\left(-\exp\left(\frac{x-\mu}{\sigma}\right)\right), & \text{if } \gamma = 0 \\ \exp\left(-\left(1 + \gamma \frac{x-\mu}{\sigma}\right)^{-1/\gamma}\right), & \text{if } \gamma \neq 0, \text{ with } x > \mu - \frac{\sigma}{\gamma} \text{ if } \gamma > 0 \text{ and } x < \mu - \frac{\sigma}{\gamma} \text{ if } \gamma < 0 \end{cases} \quad (29)$$

As discussed below, the Gumbel distribution (Gumbel, 1935, 1941), as a special case in (29) with extreme value  $\gamma = 0$ , is an appropriate model. The scale parameter is  $\sigma$ , location parameter is  $\mu$ . The local hazard function (13,14) can be derived directly from estimated variant of (29) according to the link between extreme value distribution and exceedance frequency (16); the accent symbolizes the point estimation)

$$\hat{T}(x) = 1/\hat{\Lambda}(x) = \exp\left(\frac{x-\hat{\mu}}{\hat{\sigma}_{cor}}\right) \quad (30)$$

We apply the Maximum likelihood method for the parameter estimation (Clarke, 1973, Coles, 2001, Section 2.6.3). The incompleteness of wind records per half season have been considered in the ML estimates by a modification of the procedure as explained in the Supplementary, Section 5. A Monte Carlo simulation confirms the good performance of our modification. The biased estimate of  $\sigma$  for our sample size  $n = 40$  was also detected which we considered  $\hat{\sigma}_{cor} = \hat{\sigma}/0.98$  as corrected estimation. Landwehr et al. (1979) have already stated such bias. A further bias was discovered, the EF is well estimated by (30) in contrast to the RP  $\hat{T}$ , this is strongly biased. We also corrected this as documented in the Supplementary, Section 6. The analyzed half-season maxima, record completeness and parameter estimates are listed in Supplementary Data, Table 4, 5 ad 6.

We have validated the sampling of block maxima per half season. The opportunity of correlation between the first and second half-season maxima has been tested, for significant level  $\alpha = 5\%$  around 6% fails the test with Fisher's z-transformation (Upton and Cook, 2008). This corresponds to the error of the first kind and is interpreted as correlation not being significant. Similarly, the Kolmogorov-Smirnov homogeneity test rejects 4% of the sample pairs first half to second season half season for a significant level of 5%. This 5% are the expected share of falsely rejected correct models – the first kind of error (type I error, e.g. Lindsey, 1996, Section 7.2.3).

To optimize the intensity measure of the hazard model, we have considered the wind speed with power 1, 1.5, and 2 as the local event intensity in a first fit of the Gumbel distribution by the maximum likelihood method. According to these, power 1.5 offers the best fit of wind gust data to the Gumbel distribution. Such wind measure variants were already suggested by Cook (1986) and Harris (1996).

We do not apply the generalized extreme value distribution in (24) with extreme value index  $\gamma \neq 0$  but the Gumbel case with  $\gamma = 0$  for the following reasons. At first, an extensive physical explanation would be required if some wind stations are



680 concerned by a finite upper bound for  $\gamma < 0$  and other stations not with  $\gamma \geq 0$  according to (29). Why should be local wind  
hazard short tailed for some wind stations and heavy tailed for others? River discharges at different gauging stations could  
imply such physical differences since there variants with laminar and turbulent stream (catchword Reynolds number) or very  
different retention/storage capacities of catchment areas (e.g., Salazar et al. 2012). Such significant physical differences do not  
685 exist for wind stations which are placed and operated under consideration of rules of meteorology (World Meteorological  
Organization, 2008, Section 5.8.3) to provide homogeneous roughness condition due to generate comparable data. Besides,  
we also found several statistical indications for our modelling. Information criteria AIC and BIC (Lindsey, 1996; here over all  
stations) indicate that the Gumbel distribution is the better model than the variant with a higher degree of freedom. Furthermore,  
the share of rejected Gumbel distributions of the Goodness-of-fit test (Stephens, 1986, Section 4.10) is with 6% around the  
defined significance level of 5% (the error of 1<sup>st</sup> kind – falsely rejected correct models). We have also estimated  $\gamma$  for each  
690 station and got a sample of point estimates. The sample mean of is with 0.002 very close to  $\gamma = 0$  which confirms our  
assumption. Moreover, the sample variance is 0.018 which is around the same what we get for a large sample of estimates  $\hat{\gamma}$   
for samples of Monte Carlo simulated and Gumbel distributed random variables ( $n = 40$ ). All statistics validate the Gumbel  
distribution.

## 5.2 Modelling and estimation of vulnerability

695 To quantify the loss ratio  $L_R$  at location (wind station)  $j$  and event  $i$  in the loss aggregation (26), we use the approach of Klawe  
and Ulbrich (2003) for Germany. The difference to the origin is not significant. The event intensity  $x$  is the maximum wind  
gust speed.  $v_{98\%}$  is the upper 2% percentile from empirical distribution of all local wind records. The relation with vulnerability  
parameter  $a_L$  is

$$L_{R,i,j} = a_L \text{Max}\{0, (v_{i,j} - v_{98\%})\}^3 \quad (31)$$

700 Donat et al. (2011) have used a similar formulation but with an additional location parameter. This is discarded here since the  
loss ratio must be  $L_R = 0$  for local wind speed  $v < v_{98\%}$ . This is also a reason, why a simple regression analysis (Fahrmeir et  
al., 2013) is not applied to estimate  $a_L$ . We formulate and use estimator

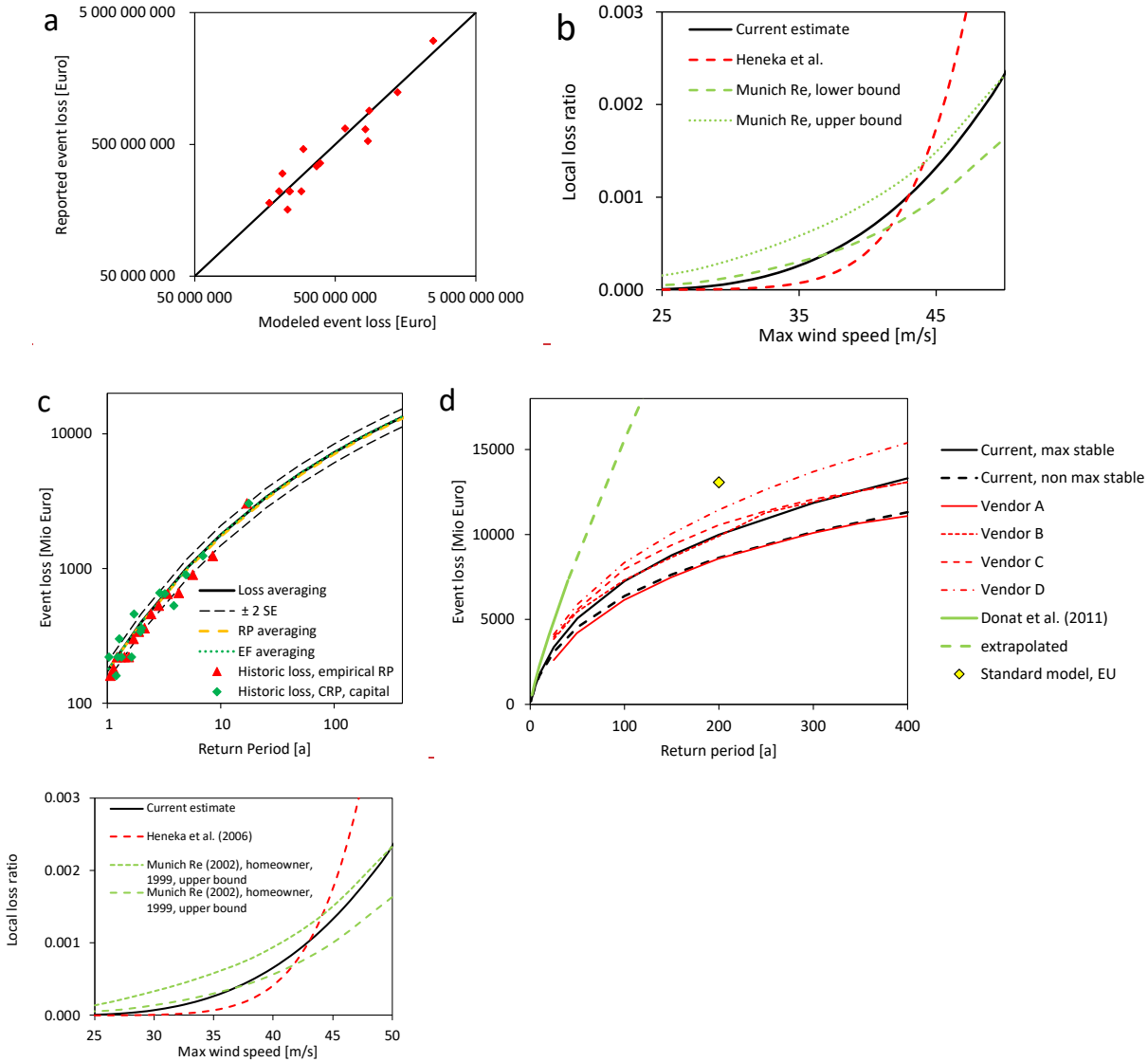
$$\hat{a}_L = \frac{1}{n} \sum_{i=1}^k \frac{\sum_{j=1}^n E_{j,i} \text{Max}\{0, (x - x_{98\%})\}^3}{L_{E \text{ reported}, i}} \quad (32)$$

with  $k$  historical storms, corresponding reported event losses  $L_E$ ,  $n$  wind stations, and local exposure value  $E_{j,i}$  being assigned  
705 to the wind station.  $E_{j,i}$  be fixed for every station  $j$  if there were wind records for every storm  $i$  at each station  $j$ . However, the  
wind records are incomplete and the assumed TSI must be split and assigned to the stations a bit differently for some storms.  
The exposure share of the remaining stations is simply adjusted so that the sum over all stations remains the TSI.

Our suggested estimator (32) has the advantage that it is less affected by the issue of incomplete data (smaller events with  
smaller losses are not listed in the data) than the ratio of sums over all events, and the corresponding standard error can be  
710 quantified (as for the estimation of an expectation). The current point estimate is  $\hat{a}_L = 9.59\text{E-}8 \pm 5.97\text{E-}9$ .

An example of our vulnerability function (with average of  $v_{98\%}$  over the wind stations) is depicted in Figure 8 and compared with previous estimates for Germany. It is in the range of previous models. Differences might be caused by different geographical resolutions of corresponding loss and exposure data. A power parameter of 2 in (31) might also be reasonable since the wind load of building design codes (European Union, 2005, Eurocode 1) is proportional to the squared wind speed. The influence of deductibles (Munich Re, 2002) per insured object is not explicitly considered but smoothed in our approach.

715



720

**Figure 8: Estimates for insured losses from winter storms in Germany: a) comparison of event losses, b) Vulnerability functions (current estimate with average of local parameters, previous estimates by Heneka and Ruck (2008) and Munich Re (2002) for residential buildings in Germany), c) current risk curves and observations, d) influence of asymptotic behavior of spatial dependence and comparison to (scaled) previous estimates (Donat et al., 2011; Waisman, 2015) and methods (European commission, 2014).**

### 3 Secondary Methods in the Analysis of German Winter Storms

#### 3.1 Modeling of local hazard

725 The local hazard curve for the EF of local event intensity must be estimated to compute the local RP by event and station for our example—winter storm over Germany. For this purpose, the relation between local event frequency and CDF of corresponding block maxima is used according to equation (3) and (6). We model the CDF of local block maxima of intensity by the Gumbel distribution. This is a special case of generalized extreme value distribution (Coles, 2001; Beirlant, et al. 2004) with extreme value index  $\gamma = 0$  in the CDF

$$730 \quad G(x) = \frac{\exp\left(-\exp\left(\frac{x-\mu}{\sigma}\right)\right), \text{ if } \gamma = 0}{\exp\left(-\left(1 + \gamma \frac{x-\mu}{\sigma}\right)^{-1/\gamma}\right), \text{ if } \gamma \neq 0}$$

(12)

#### 5.3 Numerical procedure of scaling

735 We briefly explain here the numerical procedure to calculate a risk curve via averaging the event loss. For any supporting point of a risk curve during an event loss averaging, the ELRP  $T_E$  is defined and determine the scaled CRP  $T_{cs}$  for all historical events. For each historical event, the scaling factor is  $S = T_E / T_c$  according to (24) and is applied in (27) together with local hazard function (30) and its invers. The hazard parameters are listed in the Supplementary Data, Table 4. For the scaled local intensity, the local loss ratio  $L_{R,i}$  is computed with vulnerability function (31). The corresponding parameter  $v_{98\%}$  is also listed in the Supplementary Data, Table 2. The local loss ratio  $L_{R,i}$  and the local exposure value  $E_i$  are used in (26) to compute the event loss. The considered values of  $E_i$  per event are listed in Supplementary Data, Table 7. The incompleteness of wind observation is considered therein. Finally, for the supporting point, the modelled event losses of all scaled historical events are averaged according to (28).

745 The historical events are also scaled for a defined event loss and the corresponding scaled CRP is averaged. However, the Goal Seek function in MS Excel is applied to find the correct scaled CRP  $T_{sc}$  and corresponding scaling factor  $S$ . For the averaging of the exceedance frequency, the reciprocal of  $T_{sc}$  is averaged. All these apply to max-stable scaling. For the non-max-stable scaling the scaling factor  $S$  is adjusted to a local variant according to the description in the Supplementary, Section 7. Therein, the factor  $S$  is adjusted for each station and depends on the relation of local RP to CRP of the historical event. This adjustment is made for each historical storm individually.

#### 5.4 Error propagation and uncertainties

750 The uncertainty of the local hazard models influences the accuracy of the CRP since the CRP is an average of estimates of local RP. The issue is that there is a certain correlation between the estimated hazard parameters of neighboring wind stations. We consider this by application of the Jack-knife method (Effron and Stein, 1986). According to these, the mean squared error (MSE, which is the standard error if the estimate is bias free as we assume here) of the original estimated parameter  $\hat{\theta}$  is (accents symbolize estimations)

$$755 \quad MSE(\hat{\theta}) = \sqrt{\frac{n-1}{n} \sum_{i=1}^n (\hat{\theta}_{-i} - \hat{\theta})^2}, \quad (33)$$

with the estimates  $\hat{\theta}_{-i}$  for the Jack-knife sample  $i$  of observations, being the original sample but without one of the observations/realizations. Therefore, it is also called also called leave-one-out method. The estimator (33) implies a parameter sample of  $\hat{\theta}_{-i}$  of size  $n$ , with one estimated parameter or parameter vector for each Jack-knife sample  $i$  of observations.

760 To consider any correlation in the error propagation of CRP estimate, the maximum of the same half-season  $i$  is left out synchronously when the parameter sample is computed for each wind station. Without changing the order in the parameter sample of each wind station, the CRP  $\hat{T}_{c-i}$  of the concrete historical event is computed with the hazard parameters  $\hat{\theta}_{-i}$  of each station. Finally, for this storm, the standard error of point estimate  $\hat{T}_c$  is computed according to (33).

765 We use the same approach to consider the error propagation from local hazard models to the risk estimate for the max-stable case in Section 4.4. But the finally estimated parameter  $\hat{\theta}$  in (33) is the averaged event loss  $\hat{L}_E(T_E)$  for scaled CRP. This only covers a part of uncertainties in risk estimate. We consider two further sources of uncertainty and assume that they influence the risk estimate independently to each other. The uncertainty of loss averaging is the same as during an estimation of an expectation from a sample mean and is determined by sample variance and sample size (number of scaled events). The propagation of the uncertainty of the vulnerability parameter is computed via the delta method (Coles 2001, Section 2.6.4). The aggregated standard error is the square root of the sum of squared errors. This implies a simple variance aggregation according to the convolution of independent random variables (Upton and Cook, 2008).

770 The computed standard errors in Figure 7 b are in the range 7.5 to 8.5% of estimated event loss per defined ELRP. ~~The~~ scale parameter is  $\sigma$ , location parameter is  $\mu$ . For completeness, this distribution is max-stable in a univariate sense. Extreme value index  $\gamma$  is independent of the block size ( $k$  in equation (6));  $\sigma$  is independent of the Gumbel case's block size. For a sampling of block maxima, we only consider wind speed maxima of the winter storm season that we define from September to April. A shorter definition is from October to March. The differences between the resulting block maxima are not significant. To increase the sample size, we analyze the maxima of half seasons of Autumn 1999 to Spring 2019 and have 40 observations. An entire season corresponds to one year. The distinction between block size (number of unit periods in (6)) were considered in the post-processing of the results. There is the opportunity that other kinds of wind perils contaminate our sample. As a specific compensation, extratropical cyclones also (albeit rarely) occur outside our sampling periods.

780 We consider records of wind stations in Germany of DWD (2020; FX\_MN003, a daily maximum of wind peaks, usually  
 wind gust speed [m/s]) that include minimum record completeness for one of the analyzed storms of 90%, at least 90%  
 completeness for all seasons and 55% minimum completeness per (half) season. Therefore, we only use records of 141 stations.  
 The autocorrelation between the subsequent half season maxima has been tested, for significant level  $\alpha = 5\%$  around 6% fails  
 the test. This corresponds to the error of the first kind what is interpreted that autocorrelation is not significant. Similarly, the  
 785 homogeneity test (two sample test; Conover, 1971) rejects 5% of the pairs of samples first season half versus second season  
 half for a significant level of 5%. Besides, we have considered the wind speed with power 1, 1.5, and 2 as the intensity in a  
 first fit of the Gumbel distribution by the maximum likelihood method (Coles, 2011). According to these, power 1.5 offers the  
 best fit of wind gust data. Such wind measure adjustment was already suggested by Cook (1986) and Harris (1996).

We do not consider the generalized extreme value distribution with index  $\gamma \neq 0$  in (12) for the following reasons. It would  
 790 require an extensive physical explanation if some wind stations are concerned by a finite upper bound for  $\gamma < 0$  and other  
 stations not with  $\gamma \geq 0$ . Besides, information criteria AIC and BIC (Lindsey, 1996) indicate that the Gumbel distribution is  
 the better model. In addition, the share of rejected Gumbel models (one by station) of the Goodness of fit test (Stephens, 1986)  
 is with 6% around the defined significance level of 5%, the error of 1st kind—falsely rejected correct models. Also, when we  
 estimate the extreme value index  $\gamma$ , then the standard deviation of all estimates equals the SE for estimates for actual index  
 795  $\gamma = 0$  for the same sample size. All statistics indicate the Gumbel distribution.

Even though we considered only stations with a high level of record completeness, not every sample is complete; some  
 daily records are missed. This affects the sampling of block maxima and indirect likelihood (ML) estimation for their CDF.  
 This is considered in the estimates as explained in the Supplementary. An extensive Monte Carlo simulation with 100,000  
 repetitions for sample size  $n = 40$  has been done to validate the correction's performance. We also realized that complete and  
 800 incomplete samples result in a biased estimate of  $\sigma$ ; it is only 98% of the actual value. This ML method's bias for small sample  
 sizes is already stated by Landwehr et al. (1979) and is corrected for our application. Furthermore, EF  $A(x)$  estimates for a  
 defined intensity level  $x$  are (more or less) unbiased. This does not apply to the estimated RP as reciprocal of EF (parameters  
 corresponds to (12))

$$\hat{r}(x) = 1/\hat{A}(x) = \exp\left(\frac{x-\hat{\mu}}{\hat{\sigma}_{\text{eff}}}\right) \tag{13}$$

Via the estimation results of the Monte Carlo simulation, a correction function for the local RP estimates has been derived  
 and is presented in the Supplementary. The correction function is also applied to estimates for sample size  $n = 39$  because of  
 810 the small difference. The smaller sample is applied to estimate the SE of CRPs by the leave one out method, also called  
 Jackknife method (Lindsey, 1996).

### 3.2 Modeling of vulnerability

To quantify the loss ratio  $L_{R,j}$  at location (wind station)  $j$  and event  $i$ , we use the approach of Klawa and Ulbrich (2003) for Germany. The difference to the origin is not significant. However, our variant has a bit higher correlation between reported and modelled loss. The event intensity  $x$  is the maximum wind gust speed.  $v_{98\%}$  is the upper 2% percentile from empirical distribution of all local records. The relation is with parameter  $a_L$

$$L_{R,i,j} = a_L \text{Max}\{0, (v_{i,j} - v_{98\%})\}^3,$$

(14)

Donat et al. (2011) have also used this approach but with an additional location parameter. This is discarded here since the loss ratio must be  $L_{R,j} = 0$  for local wind speed  $v = 0$ . This is also a reason, why a simple regression analysis (Lindsey, 1996) is not applied to estimate  $a_L$ . We use

$$\hat{a}_L = \frac{1}{n} \sum_{i=1}^k \frac{\sum_{j=1}^n E_{j,i} \text{Max}\{0, (x - x_{98\%})\}^3}{L_{E \text{ reported}, i}}$$

(15)

with  $k$  historical storms, corresponding reported event losses  $L_E$ ,  $n$  wind stations, and (here modelled) local exposure value  $E_{j,i}$  being assigned to the wind station. It would be the same for every station if there were wind records for every storm at each station. However, the wind records are incomplete and the assumed TSI must be split and assigned to the stations a bit differently for some storms. The normal share per station is pre-estimated by capital grid values of GAR data (normalized that sum is 1). These have been assigned to the station by the shortest distance. Our estimate for the scale parameter by (15) is  $0.0960 \pm 0.0060$ . The power parameter (exponent) and upper 2% percentile in (14) are defined and influence the risk estimate. A higher power parameter would result in higher event losses for higher RP. However, an exponent larger than 3 is not likely since an exponent of 2 would be also reasonable according to building codes (European Union, 2005) with proportional relation between squared wind peaks and structural load.

### 3.3 Error estimate and accuracy

The SE of the winter storm risk estimate for Germany is only computed for the RP-scaling (loss averaging). Thereby we consider three components. The uncertainty from the local hazard estimates is considered by the Jackknife method, applied synchronously by half season for all wind stations to consider the correlation between the SE of different stations. The SE for the vulnerability function's scaling parameter in (14) and (15) is computed as the standard error of expectation being estimated

by the sample mean. The same applies to the loss estimated by scaled CRP of 16 historical storms. The three SE are combined under the assumption of independence as the sum of their corresponding variances (square of SE).

The shares of uncertainty components on the error variance (squared SE) of our risk estimates depend on the RP. On average ~~offor~~ our supporting point, these are 15% for the limited sample of scaled historical events, 24% for the uncertainty of local hazard parameters, and 61% by the vulnerability model's parameter. We do not know a published error estimation for a vendor model for risk from winter storm over Germany and can only compare our estimates with these of Donat's et al. (2011). Their confidence range indicate a smaller precision than ours.

~~Our two weighting variants for Winter Storms over Germany correlate much better with Kendall's  $\tau = 0.814$  and Spearman's  $\rho = 0.946$  than the RPs of Della Marta's<sup>9</sup> et al. event measures for European windstorms. The accuracy of the current RP estimates is also slightly higher than these of Della Marta et al. For instance, an estimated RP 15-20 years has a SE smaller than two years currently; Della Marta et al. report RP a range of 14 years for the 95% confidence interval. This is approximately equivalent to SE of more than three years. The current precision of the German storm risk estimate with a sample of 16 historical storms is also higher than the estimates by Donat et al. (2011) with a sample of 30 historical storms.~~

### **3.45.5 RP of vendor's risk estimate**

We ~~compare~~have compared our results with vendor models in Section 4.4. These have estimated the risk curve for the maximum event loss within a year. This is a random variable, and their pseudo-RP is the reciprocal of the exceedance probability. ~~This pseudo RP and~~ can never be smaller than 1. Under the assumption of a Poisson process, we transform the pseudo RP to an actual and event related one bywith the relation between EF and ~~CF~~FCDF in ~~(6-13,16)~~. With increasing event loss, the difference between its pseudo RP and the actual ~~one~~ELRP converges to 0. The ~~concrete name of the vendors can be found in Waisman's (2015) publication. The reader should be aware that the vendors might have updated their winter storm model~~relative differences are around 5% for Germany in the meantimeELRP 10 years and 0.5% for 100 years.

## **4 Remarks on risk estimate by averaging**

### **4.1 Details of the procedure**

~~Our estimation variants are formulated by (11). For the concrete computation, elements and steps are depicted in the schemes in Figure 4 and Figure 5.~~

1. Determining scaled CRP by selection of RP of event loss  $T_{CS} = T_E$
2. Loop A – for each historical event  $i$ 
  3. Scaling factor  $S_i = T_{C,i}/T_E$  according to (9)
  4. Loop B – for each wind station  $j$ 
    5. For non-max-stable case scaling correction by  $S_{j,i} = \exp(a_j \ln(S_i)^2 + b_j \ln(S_i) + c_j)$  and  $S_{j,i} = S_i^{1+c_j T_{j,i}/T_{C,i}}$
    6. Scaling of local RP by  $T_{S,j,i} = T_j S_i$  for max-stable case, otherwise by  $T_{S,j,i} = T_j S_{j,i}$ ,  $T_{j,i}$  –RP of historical storm  $i$  at station  $j$
    7. Inverse bias correction of scaled local RP by higher solution value for  $T_{bias S,j,i}$  in  $\ln(2 T_{S,j,i}) = -0.00742 \ln(2 T_{bias S,j,i})^2 + 0.97920 \ln(2 T_{bias S,j,i}) - 0.01356$  with factor 2 since half seasons are sampled and full seasons/years are modelled
    8. Computing local event intensity by inverse of local hazard function  $x_{j,i} = \hat{\sigma}_{cor,j} \ln(T_{bias S,j,i}) + \hat{\mu}_j$
    9. Transfer of event intensity to pure wind speed  $v_{j,i} = x_{j,i}^{2/3}$
    10. Computing local loss ratio  $L_{R,i,j} = \alpha_i \text{Max}\{0, (v_{j,i} - v_{98\%j})\}^3$
    11. Computing local loss  $L_{E,i,j} = L_{R,i,j} E_{j,i}$
    12. Aggregation of local loss  $L_{E,i} = \sum_{j=1}^n L_{E,i,j}$  during loop B
- End of Loop B
- End of Loop A
13. Risk estimation by averaging of losses  $\hat{L}_E(T_E) = \frac{1}{n} \sum_{i=1}^n L_{E,i}$

**Figure 4: Computation elements and steps for RP scaling—loss averaging.**

1. Determining event loss  $L_E$
2. Loop A – for each historical event  $i$ 
  3. Numerical goal seek for scaling factor  $S_i$  and which result in determined event loss  $L_E$
  4. Corresponding RP  $T_{CS,i} = S_i T_{C,i}$
  5. Loop B – for each wind station  $j$ 
    6. Scaling of local RP by  $T_{S,j,i} = T_j S_i$ ,  $T_{j,i}$  –RP of historical storm  $i$  at station  $j$
    7. Inverse bias correction of scaled local RP by higher solution value for  $T_{bias S,j,i}$  in  $\ln(2 T_{S,j,i}) = -0.00742 \ln(2 T_{bias S,j,i})^2 + 0.97920 \ln(2 T_{bias S,j,i}) - 0.01356$  with factor 2 since half seasons are sampled and full seasons/years are modelled
    8. Computing local scaled event intensity by inverse of local hazard function  $x_{j,i} = \hat{\sigma}_{cor,j} \ln(T_{bias S,j,i}) + \hat{\mu}_j$
    9. Transfer of event intensity to pure wind speed  $v_{j,i} = x_{j,i}^{2/3}$
    10. Computing local loss ratio  $L_{R,i,j} = \alpha_i \text{Max}\{0, (v_{j,i} - v_{98\%j})\}^3$
    11. Computing local loss  $L_{E,i,j} = L_{R,i,j} E_{j,i}$
    12. Aggregation of event loss  $L_{E,i} = \sum_{j=1}^n L_{E,i,j}$  of event  $i$  during loop B
- End of Loop B
- End of numerical goal seek, if  $L_{E,i}$  equals the determined values
- End of Loop A
13. Risk estimation by averaging of RP  $\hat{T}_E(L_E) = \frac{1}{n} \sum_{i=1}^n T_{CS,i}$  or EF  $\hat{\Lambda}_E(L_E) = \frac{1}{n} \sum_{i=1}^n 1/T_{CS,i}$

**Figure 5-Computation elements and steps for Loss scaling—RP or EF averaging (only for the max-stable case).**

870

## 4.2 Stochastic background and interpretation

The estimation is based on following stochastic relations and assumptions (or proxies)

$$T_E(L_E) = E[T_{CS}(L_E)], L_E(T_E) = E[L_E(T_{CS} = T_E)], \text{ and } A_E(L_E) = E[1/T_{CS}(L_E)],$$

(16)

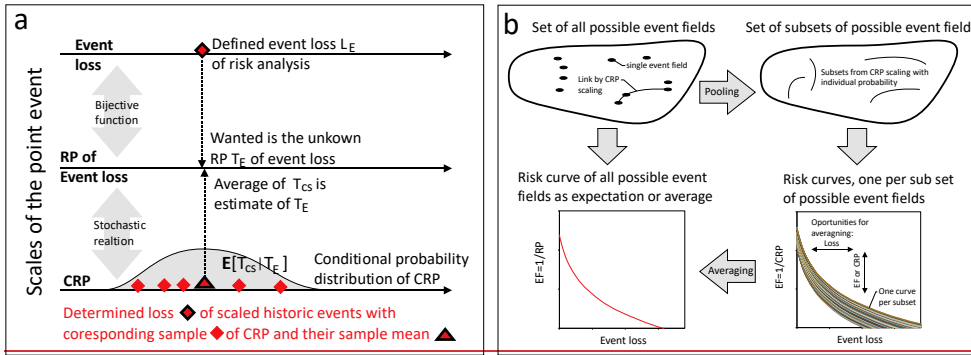
875

The origin is (5); the well-known delta method (Coles, 2011) for computation of propagation of errors is also a base. A more illustrative explanation is provided for the loss scaling by Figure 6 a. The sample mean (sample average) of corresponding CRPs is the estimate for their expectation and thereby the estimate of RP of event loss. Figure 6 b offers a further stochastic interpretation. The basic set includes all possible events which match with the risk curve. In addition, every possible wind field has a CRP. This also provides a link between some of the possible event fields—the CRP scaling and pools wind fields to subsets. The actual probability density of an observation of a random variable is mostly not known. In the same way, each “observed” subset has an unknown probability (density). And each subset corresponds to a risk curve. Their expectation

880



determines the risk curve of the entire set of event fields and is estimated by the average of a sample of linked event fields since the expectation of a random variable is estimated by the corresponding sample mean. Three averaging variants are possible.



885 **Figure 6: Schemes of the scaling-averaging approach: a) Averaging of CRP in relation to the different scales of NatCat as point event, and b) set of possible event fields as set of subsets with corresponding risk curves.**

## 56 Conclusion, discussion, and outlook

### 56.1 General

890 CRP opportunities prove once again that mathematical statistics and stochastic is the central technology for analysis, modeling, and understanding risks such as NatCat. The CRP is a simple, In the beginning, we asked the questions about the RP of a hazard event in a region, the corresponding NatCat risk, and necessary conditions for a reasonable NatCat modelling. To answer our questions, we have mathematically derived the CRP of a NatCat generating hazard event from previous concepts of extreme value theory, the pseudo polar coordinates (17). This implies the important fact that the average of the RPs of random point events remains a RP with exceedance frequency (8, 15). Furthermore, we extended Schlatter's 1st theorem for max-stable random fields to non-max-stable spatial dependence and characteristic. We have also considered the normalized variant of the area function of all local RP of the hazard event in a region with parameters CRP and CV. The absence of max-stability in the spatial dependence results in correlation between CRP and CV, which is a further indicator for non-max-stability beside changes of measures for spatial dependence by changed block size (e.g., annual maxima versus two years maxima).

895 The derived CRP is a simple, plausible, and testable stochastic measure for a catastrophe. In addition, hazard and NatCat event. The weighting of local RP in the computation of the CRP can be used to compensate an inhomogeneous distribution of corresponding measuring stations if the physical-geographical hazard component of a NatCat, the event intensity field, is of interest. However, the concentration of human values in the geographical space could also be considered in the weighting to get a higher association of the CRP with the ELRP of a risk curve. This link implies the conditional expectation (18) under the assumption of max-stable association between CRP and ELRP and offers the new approach offers the opportunity to estimate risk curves, the bijective function event loses to ELRP, via a stochastic scaling of historical intensity fields and averaging of

900

905

~~corresponding risk parameters. The averaged parameters can be the scaled CRP for a defined event fields under stochastic control. By this and a simple exposure and vulnerability model, the risk curve for loss, corresponding exceedance frequency, or the event loss for a defined/scaled CRP.~~

910 ~~The differences between the three estimators are small in our application example, insured losses from winter storm losses in over Germany could be derived. In contrast to this, the influence of the stochastic assumptions regarding spatial dependence and characteristic (max-stable or not) is significant in the range of higher ELRP. This highlights the importance of realistic consideration of spatial dependence and characteristic of the hazard in a NatCat model. Besides, our risk curves for Germany have a similar course as these those derived by vendors (Figure 7 d). The risk assumption by EU for Germany with RP 200 years is significantly higher than ours. The estimate by Donat et al. (2011) differs significantly and seems to be implausible-~~  
915 ~~for higher RP. A reason might be their statistical modeling/modelling by the generalized Pareto distribution as already applied for wind losses by Pfeifer (2011/2001). The tapered Pareto distribution (Schoenberg and Patel, 2012), also called tempered Pareto distribution (Albrecher et al., 2021), or a similar approach (Raschke, 2020) is provide more appropriate proxy/proxies for our risk curve's tail.~~

920 ~~According to our results, necessary conditions for an appropriate NatCat modelling are the realistic consideration of local hazard and their spatial dependence (max-stable or not?). Correspondingly, the spatial characteristic of NatCat events, described here by relation CRP to CV, must be reproduced. In addition, the CRPs of a simulated set of hazard events in a NatCat model should have an empirical exceedance frequency that follows the theory (15). That the standard error of an estimate should be quantified, the sampling should be appropriate, and overfitting should be avoided (catchwords over parametrization and parsimony), applies to all scientific models with a statistical component (e.g., Lindsey, 1996).~~

925 ~~The advantage of our approach over classical-vendor models for winter storm risk is the simplicity and clarity about the stochastic assumptions. Probabilistic-vendor models~~The numerical simulations for models in insurance industry (Mitchell-Wallace et al., 2017, Section 1.8) and science (e.g., Della-Marta et al., 2010) need tens of thousands of simulated storms  
(~~Mitchell-Wallace et al. 2017~~) with unpublished or even unknown (implicit) ~~stochastic assumptions on hazard and loss estimates for a defined RP.~~ We have only scaled 16 event fields of historical storms with controlled ~~stochastic~~  
930 ~~(probabilistic)stochastics~~ and could even quantify the SE. ~~The three variants of averaging result in remarkably similar outcomes-standard error.~~

~~A reasonable weighting for the CRP might depend on the examined peril. The expected annual sum of local losses might be a universal weighting since the sum of local expectations determines the expectation of total annual loss. The various weighting opportunities also underline the fact that there is not an absolute view on hazard and risk.~~

## 935 **5.6.2 Requirements of the new ~~approach~~approaches**

Our approach to CRP is based on two assumptions. At first, the local and global events occur as a Poisson process. This is ~~frequently used~~ a common assumption or approximation in extreme value statistics ~~and its application~~ (Coles, 2001) ~~and~~  
~~Chapter 7) and the corresponding Poisson distribution of number of events~~ can be statistically tested (Stephens, 1986; ~~Section~~

4.17). Moreover, the ~~detected~~verified clustering (overdispersion) of winter storms over Germany (Karremann et al., 2014) is statistically not relevant for higher RP (Raschke, 2015). With increasing RP, the number of occurring winter storms converges to a Poisson distribution. Clustering is also influenced by the event definition, which is not the topic here (catchword declustering; Coles, 2001). We also point out that the assumed Poisson process needs not be homogenous during ~~the~~ defined unit period (year, hazard season, or half-season).

The second prerequisite is robust knowledge about the local RP by a local hazard curve. ~~As it is described in Section 3, the statistical estimation is not trivial since bias correction can be required. The distinction between different perils, such as thunderstorms and winter storms, maybe an issue. Furthermore, there are~~ There are no appropriate and comprehensive models for the local hazard of every peril and region. For example, hail in Europe, we only know local hazard curves for Switzerland by Stucki et al., (2007) and these were roughly estimated. For flood hazard, there are public hazard maps of flooding areas for defined RP; corresponding local hazard curves are rarer.

### **5.3 The spatial dependence**

~~Our loss estimates for higher RP depend on the assumption for spatial dependency — with or without max stability. In consequence, questions arise for all NatCat models, which are based on generated event fields. Is the spatial dependence max-stable or not? Is the (implicit) dependence model sufficient? How is this validated? As far as we know, these are not well considered in previous models. The issue is only a marginal note in the book by Mitchell-Wallace et al. (2017) Raschke's et al. (2011) winter storm model for Switzerland implies max stability without a validation. Jongman's et al. (2014) model for European floods considers dependence explicitly. However, their assumptions and statistical inference are not appropriate according to Raschke (2015). In statistical journals, max stable dependence models have been applied to natural hazards without a systematic test of the dependence assumption, such as the snow model by Blanchet and Davison (2011) for Switzerland and the river flood model by Asadi et al. Furthermore, existing models for local hazard are partly questionable according to our discussion about local modelling of wind hazard from winter storms in Section 5.1. We have assumed a Gumbel case of the generalized extreme value distribution for local block maxima with extreme value index  $\gamma = 0$  for physical reasons and have validated this by several statistical indicators. Youngman's and Stephenson's (2016) modelling of winter storms over Europe implies an extreme value index  $\gamma < 0$  for the region of Germany, which means a short tail with a finite upper bound. Unfortunately, they have not depicted the spatial distribution of the corresponding finite upper bounds and does not provide a physical explanation for the spatial varying upper physical limit of wind speed maxima. The plausibility of such details in a NatCat model should be shown and discussed.~~

~~6.3 (2015) for the Upper Danube River system. The models for European winter storms (extratropical cyclones), that base on numerical simulations (Della Marta et al., 2010; Schwierz et al., 2010; Osinski et al., 2016), are subject to the same weakness; spatial dependence is not intensively validated.~~

~~In the copula based research by Bonazi et al. (2012) and Dawkins and Stephenson (2018), the local extremes of European winter storms are sampled by a pre defined list of significant events. Such sampling is not foreseen in extreme value statistics~~

(Coles, 2010). Block maxima and (declustered) POT are the established sampling methods. We have analyzed the dependence between block maxima, which are random variables. It is also possible to analyze stochastic associations between de-clustered peak over thresholds (POT, local point events), as Asadi et al. (2015). Further arguments against the extreme value sampling by a pre-defined event list: It is not ensured that all local extremes of the peril are considered since the storm list is not complete (smaller events are missed). In addition, European winter storm frequently does not cover Europe entirely. By this, paired observations are not ensured even though this is needed for the bivariate copula approach.

However, the copula approach for the dependence of random variables (Marie and Kotz, 2001) is a bit similar to our research of associated local point events. In both cases, the physical quantities of the margins are replaced by uniform quantities —uniformly distributed random variables or RPs.

#### 5.4 Opportunities for future research

Since the current model for the local hazard of winter storms over Germany results in considerable uncertainty, it should be improved in the future. This could be realized by a kind of regionalization of the hazard as already known in flood research (Merz and Blöschl, 2003; Hailegeorgis and Alfredsen, 2017) or by a spatial model as suggested by Youngman and Stephenson (2016). Besides, more wind stations could be considered in the analysis with better consideration of incompleteness in the records. An extension of the observation period is conceivable if homogeneity of records and sampling is ensured. A more sophisticated approach might be used to discriminate the ~~local~~ extremes of winter storms from other windstorm perils: at the level of wind station records. The POT methods (Coles, 2001, Section 4.3; Beirlant et al., 2004, Section 5.3) could then be used in the analysis even though the spatial sampling is complicated as stated in the introduction.

~~The vulnerability model results in the largest share of the uncertainty of our risk estimate even though the loss function's determined parameters imply further uncertainty. More and more detailed loss data can only improve this issue. Nevertheless, our loss function is reasonable according to previous models for Germany (Figure 6b). The influence of deductibles (Munich Re, 2002) per insured object is not explicitly considered but smoothed in our approach.~~

Further opportunities for improvements in the winter storm ~~modeling~~ modelling are conceivable. The event field might be more detailed reproduced/interpolated in more detail as done by Jung and Schindler (2019). They have considered the roughness of land cover at a regional scale besides further attributes. However, they did not consider the local roughness of immediate surroundings as discussed by Wichura (2009) ~~by the example of wind station Potsdam (Germany). He assumes that decreasing wind hazard for around 100 years is (also) a result of the development of vegetation and land use in contrast to the interpretation by Mudelsee (2020). However, our sampling period of 20 years should not be influenced so much by long term changes for a wind station.~~

Besides, our approach could be used for further hazards such as earthquake, hail, or river flood. The reasonable weighing would not be trivial for river flood. May be, the local expected annual flood loss would be a reasonable weighting if the final goal is a risk estimate for a region. The numerical handling of the case that an event does not occur everywhere in the researched region but has also local  $RP T = 0$  must be discussed for some perils, such as hail or river flood.

1005 We also see research opportunities for the community of mathematical statistics, especially extreme value statistics. Does  
(18) for conditional expected RP also apply to the non-max-stable case? A deeper theoretical understanding of non-max-stable  
random fields is of great interest from practitioners' perspectives. A research about the link between normalized area functions,  
(expectation versus CV;) and relationspatial dependence to distance is of great interest.could increase understanding of natural  
hazard and risk. And our construction for the non-max stable scaling is just a workaround to illustrate the consequences of  
1010 dependence characteristics; for risk models in practice, a transparent stochastic ~~models are~~construction is needed.  
Furthermore, estimation methods could also be extended and examined, such as the bias in estimates of RP. This bias might  
imply consequences for the broader research communitylocal RP.

### **67 Code and data availability**

A special code was not generated or used. Our computations had been simply carried out by MS Excel. The wind data were  
1015 downloaded from the server of German meteorological service (Deutscher Wetter Dienst, 2020). The exposure data were  
provided by UNISDR (2015). The loss data are part of the downloaded report of General Association of German Insurer  
(Gesamtverband Deutscher Versicherer, 2019). The here considered wind stations and storms considered in the paper are listed  
in Supplementary (~~Excel file~~);Data.

### **78 Author's contribution**

1020 The author has derived the theory, carried out analysis and wrote the paper. External help has been used regarding proofreading.

### **89 Competing interest**

The author ~~declare~~declares that he has no conflict of interest.

### **910 Acknowledgement**

The author thanks the ~~proofreaders~~reviewers for helpful comments.

## 1025 **References**

Albrecher, H., Araujo-Acuna, J., & Beirlant, J. Tempered pareto-type modelling using Weibull distributions. *ASTIN Bulletin*,  
51(2), 509-538. doi:10.1017/asb.2020.43, 2021.

Asadi P., Engelke S. and Davison A.C. Extremes on river networks. *Ann. Appl. Stat.* **9**, 2023-2050, 2015.

- Beirlant, J., Goegebeur, Y., Teugels, J. and Segers, J. *Statistics of Extremes – Theory and Application*. Book Series: Wiley Series in Probability and Statistics, John Wiley & Sons, 2004.
- Blanchet, J. & Davison A.C. Spatial Modelling of extreme snow depth. *The Annals of Applied Statistics* **5**, 1699-1725, 2011.
- Bonazzi, A., Cusack, S., Mitás, C. and Jewson, S. The spatial structure of European wind storms as characterized by bivariate extreme-value Copulas. *Nat. Hazards Earth Syst. Sci.* **12**, 1769-1782, 2012.
- Bormann, P. and Saul, J. Earthquake Magnitude, in *Encyclopedia of Complexity and Applied Systems Science*, 3, pp. 2473-2496, <http://gfzpublic.gfz-potsdam.de/pubman/item/escidoc:238827:1/component/escidoc:238826/13221.pdf>, 2009.
- ~~Clarke, R.T. Mathematical models in hydrology. Irrig. Drain. Pap. 19, Food and Agr. Organ. Of the U.N., Rom. 1973.~~
- Coles, S. *An Introduction to Statistical Modeling of Extreme Values*. Book Series: Springer Series in Statistics, Spinger, 2001.
- ~~Conover, W.J. Practical Nonparametric Statistics. New York: John Wiley & Sons. Pages 309–314, 1971.~~
- Cook, N.J. The Designer's Guide to Wind Loading of Building Structures. Part 1: Background, Damage Survey, Wind Data and Structural Classification. Building Research Establishment, Garston, and Butterworths, London, pp371, 1986.
- Dawkins, L.C. and Stephenson, D.B. Quantification of extremal dependence in spatial natural hazard footprints: independence of windstorm gust speeds and its impact on aggregate losses. *Nat. Hazards Earth Syst. Sci.* **18**, 2933-2949, 2018.
- De Haan, L. A spectral representation for max-stable processes. *The Annaly of Probability* **12**, 1194-1204, 1984.
- ~~De Haan, L., and Ferreira, A. Extreme value theory: an introduction. Springer, 2007.~~
- Della-Marta, P., Mathias, H., Frei, C., Liniger, M., Kleinn, J. & Appenzeller, C. The return period of wind storms over Europe. *International Journal of Climatology* **29**, 437-459, 2009.
- Della-Marta, P.M., Liniger, M. A., Appenzeller, C., Bresch, D. N, Koellner-Heck, P., and Muccione, V. Improved estimates of the European winter windstorm climate and the risk of reinsurance loss using climate model data. *Journal of Applied Meteorology and Climatology* **49**, 2092-2120, 2010.
- Deutsche Rück, *Sturmdokumentation*, [www.deutscherueck.de/downloads/sturmdokumentation/](http://www.deutscherueck.de/downloads/sturmdokumentation/), (download 2020)
- Deutscher Wetter Dienst (DWD, German meteorological service), Climate Data Centre (CDC), <https://cdc.dwd.de/portal/202007291339/index.html> (download Spring 2020).
- ~~Dey, D., Jiang, Y., and Yan, J., Multivariate extreme value analysis. In: *Extreme Value Modeling and Risk Analysis – Methods and Applications*. Ed. D. Dey and J. Yuan, CRC Press, Boca Raton, 2016.~~
- ~~Dombry, C. Extremal shot noises, heavy tails and max-stable random fields. *Extremes* 15, 129–158, 2012.~~
- Donat, M. G., Pardowitz, T., Leckebusch, G. C., Ulbrich, U. and Burghoff, O. High-resolution refinement of a storm loss model and estimation of return periods of loss-intensive storms over Germany. *Nat. Hazards Earth Syst. Sci.* **11**, 2821-2833, 2011.
- ~~Engelke, S., Kabluchko, Z. and Schlather, M. An equivalent representation of the Brown–Resnick process, *Statistics & Probability Letters* 81, 1150-1154, 2011.~~

[Efron, B., and Stein, C. The Jackknife Estimate of Variance. \*The Annals of Statistics\*, 9\(3\), S. 586–596, 1981.](#)

European Commission. Valuation and risk-based capital requirements (pillar i), enhanced governance (pillar ii) and increased transparency (pillar iii), COMMISSION DELEGATED REGULATION (EU) 2015/35 supplementing Directive 2009/138/EC of the European Parliament and of the Council on the taking-up and pursuit of the business of Insurance and Reinsurance (Solvency II), 2014.

European Union (EU). Eurocode 1: Actions on structures – Part 1-4: General actions – Wind actions. The European Union per Regulation 305/2011, Directive 98/34/EC, Directive 2004/18/EC, 2005.

[Fahrmeir, L., Kneib, T., and Lang, S. \*Regression - Modells, Methods and Applications\*. Springer, Heidelberg, 2013.](#)

Falk, M., Hüslér, J., and Reiss, R.-D. *Laws of Small Numbers: Extremes and rare Events*. Birkhäuser 3<sup>rd</sup> ed., Basel, 2011.

Gesamtverband Deutscher Versicherer (GDV, General Association of German Insurer), *Naturgefahrenreport - Serviceteil* (German, [www.gdv.de/de/zahlen-und-fakten/publikationen/naturgefahrenreport](http://www.gdv.de/de/zahlen-und-fakten/publikationen/naturgefahrenreport)), 2019.

[Gumbel, E.J. Les valeurs extrêmes des distributions statistiques. \*Annales de l'Institut Henri Poincaré\* 5, 115–158, 1935.](#)

[Gumbel E.J. The return period of flood flows. \*The Annals of Mathematical Statistics\* 12, 163–190, 1941.](#)

Guse, B., Merz, B., Wietzke, L., Ullrich, S., Viglione, A. and Vorogushyn, S. The role of flood wave superposition in the severity of large floods. *Hydrol. Earth Syst. Sci.* **24**, 1633-1648, 2020.

[Gutenberg, B., Richter, C. F.. \*Magnitude and Energy of Earthquakes\*. \*Annali di Geofisica\*, 9: 1–15, 1956.](#)

Harris, R. I. Gumbel re-visited – a new look at extreme value statistics applied to wind speeds. *J. Wind Eng. Ind. Aerodyn.* **59**, 1-22, 1996.

Hailegeorgis, T.T. and Alfredsen, K. Regional flood frequency analysis and prediction in ungauged basins including estimation of major uncertainties for mid-Norway. *Journal of Hydrology: Regional Studies* **9**, 104-126, 2017.

Heneka, P. and Ruck, B. A damage model for assessment of storm damage buildings. *Engineering Structures* **30**, 721-733, 2008.

Jongman, B., [Hochrainer-Stigler, S., Feyen, L.](#) et al. Increasing stress on disaster-risk finance due to large floods. *Nature Clim. Change* **5**, 264-268, 2014.

Jung, C. and Schindler, D. Historical Winter Storm Atlas for Germany (GeWiSA). *Atmosphere* **10**, 387, 2019.

Karremann M.K., Pinto J.G., von Bomhard P.J. and Klawa M. On the clustering of winter storm loss events over Germany, *Nat Hazards Earth Sys* **14**, 2041-2052, 2014.

[Keef, C., Tawn, J., Svensson, C. Spatial risk assessment for extreme river flows. \*J. R. Stat. Soc. C\* 58, 601–61, 2009.](#)

[Kendall, M. A New Measure of Rank Correlation". \*Biometrika\*. 30 \(1–2\): 81–89, 1938.](#)

Klawa, M. & Ulbrich, U. A model for the estimation of storm losses and the identification of severe winter storms in Germany. *Nat. Hazards Earth Syst. Sci.* **3**, 725-732, 2003.

Landwehr, M.J., Matalas, N. C. & Wallis, J. R. Probability weighted moments compared with some traditional techniques in estimating Gumbel Parameters and quantiles. *Water Resources Research* **15**, 1055-1064, 1979.

Lindsey, J. K. *Parametric statistical inference* Clarendon Press, Oxford, 1996.

- Mari, D. and Kotz, S. *Correlation and Dependence*. Imperial College Press, 2001.
- Merz, R. and Blöschl, G. A process typology of regional floods. *Water Resources Research* **19**, doi.org/10.1029/2002WR001952, 2003.
- 1100 Mitchell-Wallace, K., Jones, M., Hiller, J., and Foote, M. *Natural catastrophe Risk Management and Modelling - Practitioner's Guid*. Willey Blackwell, Chichester, UK, 2017.
- Mudelsee, M. Statistical analysis of climate extremes. Cambridge University Press, Cambridge, pp 124-129, 2020.
- Munich RE, GeoRisks Research Department. Winter Storms in Europe (II) Analysis of 1999 losses and loss potentials, 2002.
- National Hurricane Centre, Saffir-Simpson Hurricane Wind Scale, web page [www.nhc.noaa.gov/aboutsshws.php](http://www.nhc.noaa.gov/aboutsshws.php) (last  
1105 download Spring 2020).
- Osinski, R. et al. An approach to build an event set of European windstorms based on ECMWF EPS. *Nat. Hazards Earth Syst. Sci.* **16**, 255-268, 2016.
- [Papalexiou, S.M., Serinaldi, F., and Porcu, E: Advancing Space-Time Simulation of Random Fields: From Storms to Cyclones and Beyond. \*Water Resource Research\* 57, e2020WR029466, 2021.](#)
- 1110 [Perils AG. Products – Industry and Loss Database. Web presence, <https://www.perils.org/products/industry-exposure-and-loss-database>, last visit August 2021.](#)
- Pfeifer, D. Study 4: Extreme value theory in actuarial consulting: windstorm losses in Central Europa. In: R.-D. Reiss & M. Thomas: *Statistical Analysis of Extreme Values – with Applications to insurance, finance, hydrology and other fields*. 2<sup>nd</sup> Ed., Birkhäuser, Basel, 373-378, ~~2011~~[2001](#).
- 1115 [Punge, H.J., Bedka, K.M., Kunz, M. et al. A new physically based stochastic event catalog for hail in Europe. \*Nat Hazards\* 73, 1625–1645, 2014.](#)
- Raschke, M., Bilis, V. and Kröger, W. Vulnerability of the Swiss electric power grid against natural hazards. In *Proceedings of 11th International Conference on Applications of Statistics and Probability in Civil Engineering (ICASP11)*, Zurich, Switzerland, 2011.
- 1120 Raschke, M. Statistical modelling of ground motion relations for seismic hazard analysis. *Journal of Seismology* **17**, 1157-1182, 2013.
- Raschke, M. Statistical detection and modeling of the over-dispersion of winter storm occurrence. *Nat. Hazards Earth Syst. Sci.* **15**, 1757-1761, ~~2015~~[2015a](#).
- Raschke, M. Statistics of flood risk. *Nature Clim. Change* **4**, 843-844, ~~2015~~[2015b](#).
- 1125 [Raschke, M. A Statistical Perspective on Catastrophe Models. 31st International Congress of Actuaries \(ICA\), Berlin \(\[https://www.researchgate.net/publication/325673290\\\_A\\\_statistical\\\_perspective\\\_on\\\_catastrophe\\\_models/link/5b1ccb60aca272021cf47c03/download\]\(https://www.researchgate.net/publication/325673290\_A\_statistical\_perspective\_on\_catastrophe\_models/link/5b1ccb60aca272021cf47c03/download\)\), 2018.](#)
- Raschke, M. Alternative modelling and inference methods for claim size distributions. *Annals of Actuarial Science* **14**, 1-19, 2020.



- 130 Roberts, J. ~~et al.~~ F., Champion, A. J., Dawkins, L. C., Hodges, K. I., Shaffrey, L. C., Stephenson, D. B., Stringer, M. A.,  
Thornton, H. E., and Youngman, B. D. The XWS open access catalogue of extreme European windstorms from 1919 to  
2012. *Nat Haz Earth Sys Sci* **14**, 2487-2501, 2014.
- 135 Salazar, S., Francés, F., Komma, J., Blume, T., Francke, T., Bronstert, A., Blöschl, G. A comparative analysis of the  
effectiveness of flood management measures based on the concept of "retaining water in the landscape" in different  
European hydro-climatic regions. *Nat. Hazards Earth Syst. Sci.* **12**, 1684-9981, 2012.
- Schabenberger, O., Gotway, C.A: *Statistical Methods for Spatial Data Analysis*. Texts in Statistical Science, Chapman &  
Hall, Boca Raton, 2005.
- Schlather, M. Models for Stationary Max-Stable Random Fields. *Extremes* **5**, 33–44, 2002.
- Schwierz, C., Köllner-Heck, P., Zenklusen Mutter, E. et al. Modelling European winter wind storm losses in current and  
1140 future climate. *Climatic Change* **101**, 485–514, 2010.
- Schoenberg, F.P. and Patel, R.D. Comparison of Pareto and tapered Pareto distributions for environmental phenomena. *Eur.  
Phys. J. Spec. Top.* **205**, 159–166, 2012.
- Simth, R.L. Max-stable processes and spatial extremes. Unpublished manuscript, 1990.
- 145 Sklar, A. Fonctions de Répartition à n Dimensions et Leurs Marges. Publications de l'Institut Statistique de l'Université de  
Paris, 8, 229-231, 1959.
- Statistisches Bundesamt (German Office statistics) Preisindizes für die Bauwirtschaft – Mai 2020 (~~2020~~).
- Stephens M.A. Test based on EDF statistics. in D'Augustino, RB, Stephens, MA (Editors) *Goodness-of-Fit Techniques.  
statistics: textbooks and monographs*, Vol. 68, Marcel Dekker, New York, 1986.
- 1150 Stucki, M., & Egli, T. *Synthesebericht - Elementarschutzregister Hagel*. Präventionsstiftung der Kantonale  
Gebäudeversicherungen, ISBN 978-3-9523300-0-5, 2007.
- UNISDR, Global Assessment Report (GAR) Global exposure dataset - population and environmental built,  
<https://data.humdata.org/dataset/exposed-economic-stock>, last down load 2020, 2015.
- Upton, G. and Cook, I. *A dictionary of statistics*. 2nd rev. Ed., Oxford University Press, 2008.
- 1155 Waisman, F. European windstorm vendor model comparison (and panel discussion). In *Slides of a presentation at IUA  
catastrophe risk management conference*, London **30**,  
([https://www.iaa.co.uk/IUA\\_Member/Events/Catastrophe\\_Risk\\_Management\\_Presentations/European\\_Windstorm\\_Ven  
dor\\_Model\\_Comparison.aspx](https://www.iaa.co.uk/IUA_Member/Events/Catastrophe_Risk_Management_Presentations/European_Windstorm_Vendor_Model_Comparison.aspx)) 2015.
- Wichura, B. Analyse standortbezogener Windklimatologien als Eingangsgröße für die Bemessung von Bauwerken nach der  
DIN 1055-4. In book: *Windingenieurwesen in Forschung und Praxis* (pp.157-168) Edition: *WtG-Berichte* **11**,  
1160 Windtechnologische Gesellschaft e.V., Editor: Udo Peil, 2009.
- Youngman, B.D., and Stephenson, D.B. A geostatistical extreme-value framework for fast simulation of natural hazard  
events. *Proceedings of the Royal Society of London A: Mathematical, Physical and Engineering Sciences* **472**: 2189, 2016.

World Meteorological Organisation, *Guide to Meteorological Instruments and Methods of Observation*, . 7<sup>th</sup> Ed., WMO-  
No.8, <https://www.weather.gov/media/epz/mesonet/CWOP-WMO8.pdf>, 2008.